1967

A Search for Defect Energy Levels Produced in Czochralski Grown Silicon Irradicated with 22 Mev Protons, using Infrared Absorption Techniques

Gerald Franklin Hill
College of William & Mary - Arts & Sciences

A SEARCH FOR DEFECT ENERGY LEVELS PRODUCED IN CZOCHRALSKI GROWN SILICON IRRADIATED WITH 22 MeV PROTONS, USING INFRARED ABSORPTION TECHNIQUES

A Thesis

Presented to

The Faculty of the Department of Physics

The College of William and Mary in Virginia

In Partial Fulfillment

Of the Requirements for the Degree of

Master of Arts

By

Gerald F. Hill

January 1967

APPROVAL SHEET

This thesis is submitted in partial fulfillment of

the requirements for the degree of

Master of Arts

Gerald Z. Hill

Author

Approved, January 1967:

Harlan E. Schone

H. E. Schone, Ph.D.

George S. Orelt

G. S. Orelt, Ph.D.

H. R. Gordon, Ph.D.

ACKNOWLEDGMENT

The work reported herein is the result of a research project performed by the author as an employee of the National Aeronautics and Space Administration at Langley Research Center, Hampton, Virginia. The author is grateful to the National Aeronautics and Space Administration for allowing the results of this research project to be published as a thesis.

TABLE OF CONTENTS

LIST OF TABLES

LIST OF FIGURES

Figure Page

Figure Page

Figure Page

ABSTRACT

The techniques of infrared absorption spectroscopy were used to study the radiation effects of 22 MeV protons on silicon. Transmission spectra were obtained from 1 - 16 microns before and after irradiation. The spectra were made at both room (300° K) and liquid nitrogen temperatures (80° K). Silicon disc samples ranging in resistivity from 1.0 ohm-cm to 100 ohm-cm were irradiated to fluxes on the order of 10^{16} protons per cm^2 with 22 Mev protons. Both N-type (Phosphorous doped) and P-type (Boron doped) silicon was used in the irradiation test. All of the samples studied in this test contained a relatively high concentration of oxygen ($\sim 5 \times 10^{17}$ O_2 atoms/cm^3). They were Czochralski grown silicon samples.

Several defect levels were observed in the silicon samples. Increased absorption was observed at the wavelengths of 1.8, 3.46, 3.62, 11.6, 12.0, and 12.67 microns.

A SEARCH FOR DEFECT ENERGY LEVELS PRODUCED IN CZOCHRALSKI GROWN SILICON IRRADIATED WITH 22 MeV PROTONS, USING INFRARED ABSORPTION TECHNIQUES

INTRODUCTION

The National Aeronautics and Space Administration is very interested in the performance of semiconductor electrical components and devices when they have been subjected to a radiation environment. This interest is of course related to the fact that the space missions are very dependent upon the proper performance of many such devices for their power. As many investigators have proven, these semiconductor devices are degraded when subjected to either electromagnetic or particulate radiation (ref. 1-3). If the damage is severe enough the circuit containing the damaged component will cease functioning properly and the entire space mission may be a total loss.

There are several sources of radiation which these semiconductor devices may be subjected to in space travel. They are the Van Allen belts, solar flares, star fish, and solar winds. The first two are considered to be the most hazardous because of the large fluxes of both low and high energy electrons and protons (ref. 4-5).

The results of research efforts in the field of radiation effects on electrical components have indicated a need for a more thorough understanding of the basic mechanisms produced in a semiconductor material. This understanding may be accomplished by studying the electrical and optical properties of the basic silicon semiconductor before and after being irradiated.

Simulated space radiation conditions may be obtained for laboratory study by utilizing radiation sources such as isotopes, accelerators, and cyclotrons. There are many of these sources available to the experimenter interested in studying the radiation effects of electromagnetic and particulate radiation on components and materials. Since the major damage to semiconductors from protons occurs from particles having energies from 50 MeV and below the 22 MeV proton cyclotron at the Oak Ridge National Laboratories was used in this investigation (ref. 6).

Many investigators have studied the radiation effects of charged particles, X-rays, gamma rays, and neutrons on semiconductor materials (ref. 7-13). However, most of the studies were accomplished using particles other than protons. Very little data exist on the effects of protons on semiconductor materials.

There are several ways of assessing the damage produced in the material irradiated. The most commonly used are minority carrier lifetime studies, Hall coefficient as a function of temperature, mobility changes, electron paramagnetic resonance, photoconductivity, and infrared absorption.

The results of all of these studies are similar in that they are sensitive enough to detect defect energy levels produced within the basic semiconductor material. Many levels have been observed, however, only three have been studied in enough detail to furnish a complete understanding of the defect. These are the A-center (E_c - 0.17 ev), E-center (E_c - 0.40 ev), and the divacancy (E_c - 0.21 ev).

The use of infrared spectroscopy as a microscopic probe for the study of radiation induced defects in silicon has been shown to be an important probe by many workers (refs. 9, 14-18) in recent years. In the past, defects introduced in silicon by reactor neutrons, 9.6 MeV deuterons and electrons of various energies were observed to give rise to new infrared absorption bands in silicon in the wavelength region 1.8 to 20.5 microns. The defect bands found can be divided into two groups (ref. 14). The first group of bands is associated with electronic excitation and is located in the wavelength range 1.8 to about 6.0 microns. The second group of bands 9 to 20.5 microns are vibrational bands. In general the bands between 9 and 12.5 microns arise only from defects associated with atomically dispersed oxygen in silicon.

The research effort reported herein is the result of an investigation of the bombardment of silicon with 22 MeV protons. The techniques of infrared absorption spectroscopy was used to locate the defect energy levels produced in the material.

One cannot obtain a picture or model of the defects observed by using only one method of assessing the damage. Several methods must be used and the results compared. Therefore, it is not the purpose of this thesis to draw complete conclusions on the symmetry, and so forth, of the defect levels observed but to merely complement existing data in hopes that someone may combine all such data and form the necessary models.

CHAPTER I

THEORY

Semiconductor band theory. --- The properties of silicon semiconductor material are best explained by using band theory. The bands to be considered are the valence, forbidden, and conduction bands (see fig. 1). The valence band in silicon contains the four valence electrons. There is actually a large number of allowed energy levels in the valence band for electrons to occupy but they lie so close to each other one can speak of them as a continuum. However, each electron must occupy one of these energy levels or quantum states.

Just above the top of the valence band is what is called the forbidden band or gap. It is called the forbidden band because there are no quantum states available for electrons, therefore, they cannot exist in this region. However, allowed levels may be placed in the forbidden region by doping the silicon with impurities. This will be discussed later on in the text.

Above the forbidden gap lies the conduction band. This is a band in which electrons are free to move about and conduct current. It is also a band of many quantum states but here again they are very close to each other and may be considered as a continuum.

At absolute zero degrees the conduction band is completely empty of electrons and they occupy levels in the valence band. Therefore there can be no current at this temperature. In reality this is not the case so there is always some electrons in the conduction band.

Figure 2 (ref. 19) shows a schematic diagram of the energy bands in silicon. It is represented in k-space. One can see that silicon is an indirect energy band semiconductor. This simply says that at $k = o$ the top of the valence band does not lie directly beneath the bottom of the conduction band. Therefore, the transitions from the valence band to the conduction band are not vertical. The top of the valence band lies at $k = o$ and the energy surfaces are approximately spherical.

When discussing energy levels in semiconductors one talks of the Fermi level. The Fermi level (E_f) is a statistical level located in the forbidden gap having a probability of occupancy equal to one-half. The position of the Fermi level is dependent on the temperature and carrier concentration (resistivity). The carrier concentration is varied by adding impurities to the silicon lattice. Silicon is a group IV material. When a group V material such as phosphorous is added to silicon it produces donor levels (N-type) in the forbidden band close to the conduction band. In this case the Fermi level is shifted towards the conduction band. When a group III material such as boron is added to silicon it produces acceptor levels (P-type) in the forbidden band close to the valence band. In this case the Fermi level is shifted towards the valence band.

For a spherical energy band in a semiconductor

$$g(E) = 4\pi\left(\frac{2\,m_e}{h^2}\right)^{3/2} E^{1/2} \qquad (1)$$

where:

$E = p^2/2m$

$g(E)$ = density of states function or the number of states available per unit energy

m_e = effective mass of electron

h = Planck's constant $\left(6.625 \times 10^{-27} \text{ erg. sec}\right)$

Defining the function $f(E)$ as the probability of occupancy for a state of energy E we have the relationship:

$$f(E) = \left[1 + \beta e^{\left(E-E_f\right)/kT}\right]^{-1} \tag{2}$$

where:

β = a statistical weight factor having a value between 1/2 and 2. It is usually taken to be unity.

k = Boltzmann's constant

T = temperature

See figure 3 for a plot of the Fermi-Dirac distribution function $f(E)$ versus energy E. Using equations (1) and (2) an expression for the carrier concentration of electrons in the conduction band can be written as:

$$n = \int_{-\infty}^{+\infty} g(E)\, f(E)\, dE \tag{3}$$

$$= 2\left(\frac{2\pi\, m_e\, kT}{h^2}\right)^{3/2} e^{-\left(E_c - E_f\right)/kT} \tag{4}$$

$$= N_c e^{-(E_c - E_f)/kT} \qquad (5)$$

where:

$$N_c = 2\left(\frac{2\pi\, m_e\, kT}{h^2}\right)^{3/2} = \text{the number of states in the conduction band}$$

An expression for the position of the Fermi level for N-type material is obtained by solving equation (5) for E_f.

$$E_f = E_c - kT \ln\left(\frac{N_c}{n}\right) \qquad (6)$$

$$E_f = E_c - kT \ln\left[\frac{2(2\pi\, m_e\, kT)^{3/2}}{h^3 n}\right] \qquad (7)$$

and similarly for P-type material the position of the Fermi level can be calculated from:

$$E_f = kT \ln\left[\frac{2(2\pi\, m_p\, kT)^{3/2}}{h^3 p}\right] + E_v \qquad (8)$$

where:

m_p = effective mass of hole

p = hole concentration

Determination of oxygen content in silicon. --- All of the silicon samples used in this investigation were grown by the pulled method. This method is usually referred to as the Czochralski method. The concentration of oxygen in pulled samples $(10^{17} - 10^{18}\ O_2\ \text{atoms/cm}^3)$ is large compared to vacuum float zone grown silicon $(10^{15} - 10^{16}\ O_2\ \text{atoms/cm}^3)$. Interstitial oxygen in the silicon lattice

gives rise to an absorption band at approximately 9 microns. The relative strength of the absorption band is proportional to the oxygen concentration in the silicon lattice. Figure 4 shows a comparison of the absorption bands for pulled and float zone grown silicon at 9 microns. An interesting fact is that the area between the curves in figure 4 (corresponding to the oxygen absorption only) remains a constant. It is independent of temperature, resistivity, or conductivity type. The limit of detectability at liquid air temperature is approximately 10^{-5} weight percent oxygen or 10^{16} oxygen atoms/cm^3 (ref. 20).

Kaiser, Keck, and Lange (ref. 20) state that the quartz crucible reacts with molten silicon to form gaseous SiO. The quartz crucible is used as a container for the molten silicon. The SiO is then able to dissolve into the silicon crystal lattice to some extent. During the process of cooling down the molten silicon, it becomes crystallized and the oxygen becomes bonded to the silicon.

The number of SiO oscillators in the silicon sample may be estimated using optical measurements. If one considers N_{io} independent oscillators, having vibrational frequencies only, the area enclosed by the absorption band is given by (ref. 20):

$$\int \alpha_{\upsilon} \, d\upsilon = N_{io} \frac{\pi e^2}{3\mu c} \frac{\left(n^2 + 2\right)^2}{9n} \tag{9}$$

where:

α_υ = absorption coefficient at the frequency υ

μ = reduced mass of the SiO oscillator (10.2)

e = net electronic charge (4.8×10^{-10} esu)

n = refractive index of the surrounding medium (3.6)

c = velocity of light (3×10^{10} cm/sec)

As an approximation one can use

$$\int \alpha_\upsilon \, d\upsilon \simeq \alpha_{max} \Delta H \tag{10}$$

where:

α_{max} = absorption coefficient at the band maximum

ΔH = half width of the band

Using this approximation and solving the equation for N_{io} one obtains:

$$N_{io} \simeq \frac{9n}{(n^2 + 2)^2} \frac{3\mu c}{\pi e^2} \alpha_{max} \Delta H \tag{11}$$

Each oxygen atom is bonded to two silicon atoms forming an isosceles triangle, therefore, giving two oscillators. The corresponding oxygen concentration, O.C., is therefore given by:

$$O.C. \simeq \frac{N_{io}}{2} \tag{12}$$

$$O.C. \simeq \frac{27\, n\mu c}{2(n^2 + 2)^2\, \pi e^2} \alpha_{max} \Delta H \tag{13}$$

The oxygen concentration was calculated using this technique for all of the silicon samples used in this investigation and the results are presented in Table II.

Determination of absorption coefficient. --- The quantity usually measured with an infrared spectrometer is percent transmission. It simply records the relative amount of light transmitted versus wavelength. For a given material, for example silicon, the transmission is reduced as the thickness is increased. In many instances a comparison of sample thickness and relative absorption is needed. To accomplish this one must calculate the absorption coefficient for each sample as a function of wavelength.

The absorption coefficient, α, can be calculated from the measured transmission by means of the expression (ref. 22):

$$T = \frac{I}{I_o} = \frac{(1 - R)^2 \, e^{-\alpha x}}{1 - R^2 \, e^{-2\alpha x}} \tag{14}$$

where:

x = sample thickness

α = absorption coefficient

R = reflectivity for the wavelength at which the transmission T is measured

I_o = intensity of incident light

I = intensity of transmitted light

The above equation allows for multiple internal reflections from the silicon surfaces. This is important when the transmission and reflectivity are high. When the internal reflections are not large, $R^2 e^{-2\alpha x} << 1$, one can determine the absorption coefficient, α, from the equation:

$$T = \frac{I}{I_o} = (1 - R)^2 \, e^{-\alpha x} \tag{15}$$

Solving the above equation for the absorption coefficient one obtains:

$$\alpha = \frac{\ln \left[\frac{(1 - R)^2}{(I/I_o)} \right]}{X} \tag{16}$$

The reflectivity of a clean surface for normal incidence is determined by:

$$R = \frac{(n - 1)^2 + k^2}{(n + 1)^2 + k^2} \tag{17}$$

where:

n = refractive index of the material

k = extinction coefficient

CHAPTER II

SAMPLE PREPARATION

The silicon used in this investigation was purchased commercially in ingot form from the Texas Instruments Incorporated. All of the ingots used in this investigation were grown by the technique of being pulled from the melt in a quartz crucible. This method is referred to in the literature as the Czochralski method. Figure 4 shows the absorption at 9 microns due to interstitial oxygen in float zone grown silicon (10^{15} - 10^{16} oxygen atoms/cm^3) to be small compared to the absorption in pulled silicon (10^{17} - 10^{18} oxygen atoms/cm^3). A high oxygen concentration was desired for this investigation since it is required if the A-center is to be detected easily.

All of the N-type ingots were doped with Phosphorous and all of the P-type ingots were doped with Boron. The manufacturers supplied the value of resistivity requested to within $\pm$ 10 percent.

The ingots were approximately 10.0 cm in length and 3.0 cm in diameter. The ingots were grown in the (111) orientation. This orientation was known to within 2 degrees.

Silicon disc samples were made by slicing the ingots normal to the horizontal axis with a diamond cutoff saw. The thickness of the samples was intentionally made thicker than what was needed to allow for loss during polishing. The flat side of the discs was the (111)

plane. After slicing, the samples were given a progressive rough grind using silicon carbide grits of 180, 400, and 600. Each sample was then polished with aluminum oxide (number 302, 303, 303 1/2). Additional polishing continued with diamond compounds of 22, 8, and 1 micron sizes on a pellon lap. An optical finish was obtained using cerium oxide in the final polish with a felt lap. The thickness of the samples after polishing varied from 0.79 mm to 3.63 mm (see Table I). The samples were optically polished to increase the transmission.

CHAPTER III

DESCRIPTION OF APPARATUS

The IR-9 infrared spectrophotometer. --- The IR-9 infrared spectrophotometer (fig. 5) is capable of recording transmission spectra in the infrared region of the electromagnetic spectrum. The wavelength range is 4000 - 400 cm^{-1} (2.5 - 25 microns).

A Nernst glower is used as an infrared source. After leaving the source the radiation is chopped by a rotating mirror. One cycle passes through the sample position and the alternate cycle passes through a reference position (reference beam). From these points the radiation is incident on another rotating mirror which is synchronous with the first rotating mirror. The radiation then passes on through a double monochromator (50 cm focal length, f-10 aperature) into a permanently evacuated thermocouple (potassium bromide window). The output of the thermocouple is then amplified and recorded. Every other signal is the reference signal and is compared to the alternate signal which is proportional to the transmission characteristics of the sample at that particular wavelength. The spectrophotometer may be operated in the single beam mode also.

Some of the more important specifications are listed below:

1. Prism: potassium bromide, 60 x 75 mm, 58.2° angle.

2. Gratings: two Bausch and Lomb "Certified Precision", replica, area 64 x 64 mm; one with 50 lines/mm and 19.98 micron blaze; another with 150 lines/mm and 6.67 micron blaze.

3. Slits: bilateral; entrance, intermediate and exit simultaneously and automatically adjustable from 0 - 6 mm; height, 25 mm.

4. Resolution: 0.25 cm^{-1} at 923 cm^{-1}.

5. Frequency accuracy: ± 0.2 cm^{-1} at 400 cm^{-1}; ± 0.3 cm^{-1} at 740 cm^{-1}; ± 0.4 cm^{-1} at 1330 cm^{-1}; ± 0.5 cm^{-1} at 2220 cm^{-1}; ± 0.6 cm^{-1} at 4000 cm^{-1}.

6. Percent transmission accuracy: 0.2 percent for any single reading in single beam; 1.0 percent absolute or 0.2 percent with calibration in double beam.

7. Frequency repeatability: 0.1 percent throughout entire range.

8. Percent transmission repeatability: 1 pen width

9. Stray radiation: 0.1 percent or less at 700 cm^{-1} polystyrene band.

10. Purging: air dryer connections for purging entire system.

Low temperature cryostat. --- The low temperature cryostat (fig. 5) used in the experiment was made out of glass. It consisted of an outside shield with a liquid nitrogen well connected to a copper cold finger. A copper sample holder screws to the cold finger and gives very good conduction of heat. The outside well has a feed through for a thermocouple lead for monitoring the sample temperature. It also has an opening for a vacuum line.

Two sodium chloride windows were used to allow the infrared beam to pass through the sample. The windows are held into position with metal end plates and screws.

With a vacuum of approximately 10^{-6} torr, a sample temperature of approximately 80° K was obtained with liquid nitrogen in the well.

The DK-1A spectrophotometer. --- The DK-1A spectrophotometer (fig. 6) is capable of recording transmission spectra in the far and near ultraviolet, visible and near infrared regions of the electromagnetic spectrum. The wavelength range is 185 - 3500 millimicrons.

A tungsten source is used for the visible and near infrared regions and a hydrogen lamp is used for the ultraviolet region.

The DK-1A utilizes a single beam of energy which is chopped into alternate reference and sample beams to provide a double beam system within the sample compartment. Both sample and reference beams have common detection and amplification components. Ratio recording (comparison of sample beam energy with reference beam energy) eliminates inaccuracies due to such effects as source fluctuations; changes in amplifier gain, sensitivity, or spectral response of the detector, and the presence of common absorbing gases in the sample and reference paths. However, for specific applications the spectrometer may be used in the single beam mode. The entire system is capable of being purged.

The monochromator section is a quartz prism which has an aluminized back side such that the beam of light passes through the prism twice. After passing through the monochromator the light beam passes through

the sample position and then into an integrating sphere. This sphere is coated with magnesium oxide (MgO) and a detector is mounted on top of the sphere. A lead sulfide (PbS) cell is used as a detector for the visible and near infrared regions and a photomultiplier tube is used for the ultraviolet region.

Some of the more important specifications are listed below:

1. Resolution: better than 0.2 millimicron at 220 millimicrons.

2. Wavelength accuracy: better than 0.4 millimicron in ultraviolet, 1.5 millimicrons in visible, and 8 millimicrons in near infrared.

3. Transmission accuracy: better than 0.5 percent.

4. Wavelength reproducibility: better than 0.05 millimicron in ultraviolet and 0.5 millimicron in near infrared.

5. Transmission reproducibility: better than 0.2 percent transmittance.

6. Stray radiation: less than 0.1 percent from 210 to 2720 millimicrons.

7. Slits: entrance and exit slits simultaneously and continuously adjustable, manually or automatic, from 0 to 2.0 millimeters. The exit slit heights are 1.5, 4.0, or 12 mm selected manually.

CHAPTER IV

EXPERIMENTAL PROCEDURE

Pre-irradiation measurements. --- All of the samples used in this investigation were optically polished on both sides before any spectra were taken. After the polishing procedure the samples were cleaned with acetone and alcohol and then were left for some time to allow the liquids to evaporate.

Before any spectra on the samples were made the IR-9 and DK-1A spectrophotometers were set up to run and calibrated for wavelength. The 0 percent and 100 percent lines were taken on each instrument to determine the background absorption due to the atmosphere, etc... However, the background was found to be very constant over the wavelength range because each instrument was purged with dry air. Figure 7 shows a calibration spectrum taken with the IR-9 spectrophotometer. It was made with a thin film of polystyrene. The DK-1A was calibrated for wavelength by using a mercury pen lamp. Since this was for only one wavelength the calibration is not known.

After calibrating the IR-9 the low temperature cryostat was placed in the sample position and another 100 percent line was taken. This was also found to be constant over the wavelength region except it began to drop off at approximately 16 microns due to the characteristics of the NaCl windows used in the cryostat. During

these measurements the cryostat was evacuated and full of liquid nitrogen at all times. The cryostat was then emptied and a sample placed in the copper ring holder. A thermocouple was attached such that it was in contact with the silicon sample but not in the infrared beam. After the cryostat had been filled and allowed to stabilize at the proper temperature (80 $\pm$ 1° K as determined by a thermocouple and potentiometer) an infrared spectra was taken. In order to determine if there were any surface effects being seen, because of room light, rather than bulk effects, another spectrum was taken with the sample and cryostat covered with black cloth to keep out any light. There were no differences observed in the two spectra. Therefore, all other spectra, with exception of one made after irradiation which also was not different, were taken in the daylight. All other samples were run (2.5 - 16 microns) in this manner before irradiation.

The samples were then dried off because they became wet from the condensation as the cryostat was opened before the samples could reach room temperature. Each sample was then placed in the sample compartment of the DK-1A spectrophotometer and spectra obtained at room temperature. No liquid nitrogen temperature data was taken because of the lack of space available in the sample compartment of the DK-1A. Each spectrum was scanned from 1.0 - 3.5 microns.

Reflectance measurements were made on the DK-1A from 1.0 - 3.5 microns and was found to be essentially a constant over the wavelength region (R = 0.30).

Irradiation procedure. --- All of the samples were irradiated with 22 MeV protons. The 22 MeV protons were obtained by using the 86-inch cyclotron at the Oak Ridge National Laboratory in Oak Ridge, Tennessee. The 86-inch cyclotron has a fixed frequency of 13.4 Mc and a magnetic field of approximately 9000 gauss. The cyclotron developes a maximum internal beam current of 3000 μa at 17.5 MeV and 1500 μa at 22 MeV.

The samples were irradiated in the "T" position of the beam transport system. Figure 8 shows the "T" position and associated equipment. A sample probe was made to hold the silicon sample into position in the proton beam (fig. 9). It has provisions for water cooling and is insulated from the beam pipe so it may be used as a charge collector. The total beam current incident on the sample was monitored in this fashion. Figure 10 shows the spiral water flow assembly which holds the sample into position in the sample probe. The spiral water flow assembly allowed excellent cooling of the samples during irradiation. The sample temperature was monitored with a thermocouple and never exceeded 40° C during any of the runs.

Post-irradiation procedure. --- Immediately after irradiation all of the samples were placed in a dry ice container to prevent any excessive room temperature annealing before the spectra could be made. The samples were then brought back to the lab and infrared spectra were obtained as before irradiation.

A reflectance spectrum was made on several samples and there was no detectable difference in the pre and post-irradiation spectra. The value of the reflectance used in determing the absorption coefficient was calculated using the index of refraction, $n = 3.42$. This gave a value of $R = 0.30$ which agrees with the experimental measurement.

CHAPTER V

DISCUSSION OF EXPERIMENTAL RESULTS

Band edge. --- The existence in all semiconductors of a wide spectral region of very intense absorption, limited on the long wavelength side by a sharp edge, is due to the fact that the absorption of photons of sufficiently high energy is accompanied by electron transitions from the valence to the conduction band.

In the case of silicon, light of frequency $\nu < \frac{Eg}{h}$, where Eg is the energy width of the forbidden band, passes through pure crystals without photoionization. However, when light having frequencies of $\nu \geq \frac{Eg}{h}$ is incident upon silicon there is a strong absorption. One can use this type of spectra to calculate the energy difference, Eg, between the valence and conduction band. Figure 11 shows the percent transmission versus wavelength for a silicon sample (422 P) pre and post-irradiation. By extrapolating a tangent line from the pre-irradiation percent transmission curve down to the wavelength scale one intercepts the wavelength scale at $\lambda = 1.04\ \mu$ (microns). Using the equation

$$E = h\nu \tag{18}$$

$$E = \frac{hc}{\lambda} \tag{19}$$

$$E(ev) = \frac{1.24}{\lambda(\mu)} = Eg(ev) \tag{20}$$

and the value of $\lambda = 1.04\ \mu$ the width of the forbidden gap is calculated to be $Eg = 1.19$ ev. The band edge is seen to shift towards

the longer wavelength region (lower energy) after it has been irradiated. The reason for this shift is that radiation introduces donor and acceptor levels in the forbidden gap which decreases the energy difference between initial and final states of the electron. From figure 11 the E_g after irradiation was found to be 1.09 ev. This value is very dependent on how one draws the tangent to the post-irradiation curve. The amount of shift is a function of the exposed radiation. Fan and Ramdas (ref. 9) state that after prolonged irradiation of silicon with deuterons the radiation effect seemed to saturate after a shift of about 0.1 ev, which agrees with the results of figure 11. All of the samples irradiated in this investigation exhibited the same shifting effect.

Cheng (ref. 18) has shown, after a detailed analysis of the background absorption for the 1.8 micron absorption band, that after 45 MeV electron irradiation of silicon a new radiation induced absorption band is produced in the wavelength range from the fundamental absorption edge up to higher wavelengths. The intensity of the new absorption band increases monotonically with the increase of the photon energy. Figure 11 indicates this defect level from the overall shift and shape of the pre-irradiation versus the post-irradiation spectra.

The 1.8 micron band. --- The 1.8 μ band was first observed by Becker in neutron irradiated and deuteron irradiated silicon (ref. 9). Since then other investigators have observed the 1.8 μ band in both N and P-type silicon irradiated with electrons deuterons, neutrons, gamma rays

and this report shows that protons (22 MeV) produce the same defect level (see figures 11 - 13).

Fan and Ramdas (ref. 9) observed the 1.8 μ band in samples which had high resistivities or were P-type after irradiation. An N-type sample in which the Fermi level was approximately 0.16 ev below the conduction band did not exhibit the band. However, figure 11 shows the 1.8 μ band located in an N-type, 10 ohm - cm sample. This sample received a large dose of protons, 2.23×10^{16} protons/cm^2.

The width at half maximum for sample 422 P (fig. 11) was calculated to be 0.13 ev. This spectrum was taken at room temperature. Fan and Ramdas (ref. 9) found that the width at half maximum was 0.1 ev at 80° K and 0.16 ev at 300° K. The results of this report agree quite well with their results. All of the widths at half maximum were approximately the same for the samples exhibiting the 1.8 μ band.

Due to the size of the sample compartment in the DK-1A spectrometer a cryostat could not be placed in it to obtain low temperature results. Other investigators (ref. 9, 18) have studied the properties of the 1.8 μ band at lower temperatures and found that the band sharpens up and shifts towards the shorter wavelength region. Fan and Ramdas report that the band was absent at liquid nitrogen temperature but present at room temperature. From this result they concluded that the defect responsible for the absorption band has an energy level at approximately 0.21 ev below the conduction band and will not be seen if the level is occupied by electrons.

Figure 14 shows the percent transmission versus wavelength for sample N which was N-type, 10 ohm cm. It failed to show the 1.8 μ band. This may be explained by the fact that it received only half the dose the other samples received. It is unfortunate that electrical properties were not measured in conjunction with the optical properties so that the position of the Fermi level could be calculated. This would help in explaining the reasons for either observing or not observing defect levels.

Cheng (ref. 18) has completed an extensive study on the 1.8 μ band in 45 MeV electron irradiated silicon. From a combination of optical, electrical and mechanical properties he was able to essentially pin point the defect levels associated with the 1.8, 3.3 and 3.9 μ bands.

Watkins and Corbett (ref. 23) identified two electron paramagnetic resonance spectra (Si - G6) and (Si - G7) as arising from two different charge states of a divacancy. Figure 15 is a model of the divacancy. In this model, the two vacancies are at adjacent atom sites, labeled c and c'. The construction of the defect can be visualized as follows: initially, there are six broken bonds around the divacancy, one each for the six atoms neighboring it. Atoms a and d pull together to form a covalent bond as do atoms a' and d'. Actually, any two of the three atoms a, b, d, can pull together to form the covalent bond, it is the same for the atoms labeled with primes. From this one can see that there are three equivalent electronic distributions for a divacancy. Figure 16 shows these three combinations. The 1.8, 3.3 and 3.9 μ bands are associated with the same defect level in different charge states. The

level responsible for these bands is located at E_c - 0.21 ev. Descriptions and results of the other bands are presented in other sections of this report.

The 3.46 and 3.62 micron bands. --- The 3.46 and 3.62 micron bands have been seen by several investigators (refs. 9, 18). Both pulled and float zone grown silicon exhibit these bands, however, the production rate is higher in pulled silicon. Fan and Ramdas have observed the bands in neutron and electron irradiated samples. At room temperature the peak absorption was at 3.3 μ. However, when the temperature was lowered to liquid nitrogen temperature the peak resolved into three sharp bands located at 3.62, 3.46, and 3.3 microns. The results of my investigation are shown in figures 17 - 19. The bands seen at liquid nitrogen temperature had peak absorptions at 3.46 and 3.62 microns. Both N and P-type pulled silicon samples showed the bands (figs. 17 - 19). Fan and Ramdas (ref. 9) state that the absorptions were not present in P-type samples or N-type samples of high resistivities. However, the results of this investigation indicated the bands were produced in both P and N-type silicon. Under the illumination of light with all wavelengths, as was the case in this experiment, the elctronic distribution in the crystal would be different from that with monochromatic light, as in the experiment of Fan and Ramdas, since the electrons can be redistributed through the conduction band. Therefore, the absorptions can be observed in our case, even if the

Fermi level of the sample without illumination is lower than the level which must be populated by electrons in order to have the absorption. The level can become populated with electrons through redistribution. Also the production rate of these two bands is dependent upon the Fermi level position. This is seen to be the case because the strength of the bands in the lower resistivity samples are stronger than the bands seen in the higher resistivity samples (see figures 17 - 19). The defect level responsible for these absorptions is located at E_c - 0.21 ev. They are another charge configuration of the divacancy (ref. 18).

The 11.6, 12.0 and 12.67 micron bands. --- The 11.6, 12.0 and 12.67 micron bands were observed in all of the samples irradiated. Several investigators have found these defect levels in pulled silicon (ref. 15). The bands are only observed in oxygen containing silicon samples. Neutrons, deuterons, electrons, and gamma rays have produced the levels and the results of this investigation show that 22 MeV protons also produce the defect.

It has been shown by Watkins and Corbett (ref. 13) and Corbett, Watkins, Chrenko, and M^{c}Donald (ref. 15) using both spin resonance and infrared absorbtivity measurements that the defect configuration which is responsible for the 12 μ band is an oxygen vibrational band composed of a substitutional oxygen atom coupled to a vacancy. This defect has been called the silicon A-center (ref. 13). The temperature dependence of the 12 μ band which is reported in this report is the same found by Corbett (ref. 15) et.al. in that the absorption peak shifts to shorter

wavelengths as the temperature is lowered from room temperature to liquid nitrogen temperature.

The results of this investigation are shown in figures 20 - 22. As can be seen the defects are produced in both P and N-type silicon.

Figure 23 shows the position of the oxygen atom relative to the surrounding silicon atoms. A 9 μ band is observed when the oxygen atom is located interstitially and the A-center is observed at 12 μ when the oxygen atom is in the substitutional position. The corresponding electrical level is located at E_c - 0.17 ev (fig. 24).

CHAPTER VI

CONCLUSIONS

From the results presented herein, the following conclusions may be derived:

1. Infrared absorption spectroscopy is an excellent probe for studying radiation induced defects in semiconductors.

2. Proton (22 MeV) irradiated silicon produces defect levels in the forbidden gap similar to other particulate and electromagnetic radiation. The absorption edge shifts toward longer wavelengths with increased radiation.

3. The relative strength of the A-center, as indicated by the 12 micron absorption band, is proportional to the oxygen concentration in the sample. Infrared absorption can easily be used to estimate the oxygen concentration in silicon.

4. Although all of the room temperature data is not presented, the infrared spectra obtained with the samples at lower temperatures are sharper and more distinct.

REFERENCES

1. Beatty, M. E.; and Hill, G. F.: NASA TN D-2817 (1965).
2. Honaker, W. C.; and Bryant, F. R.: NASA TN D-1490 (1963).
3. Hulten, W. C.; Honaker, W. C.; and Patterson, J. L.: NASA TN D-718 (1961).
4. Foelsche, T.: NASA TN D-1267
5. McDonald, F. B.: NASA TR R-169 (1963)
6. Oliver, J. W.: Space Technology Lab. Inc., MR-16 (8987-0001-RU,001), February 19, 1962.
7. Bemski, G.: J. Appl. Phys. 30, 1195 (1959).
8. Watkins, G. D.; Corbett, J. W.; and Walker, R. M.: J. Appl. Phys. 30, 1198 (1959).
9. Fan, H. Y.; and Ramdas, A. K.: J. Appl. Phys. 30, 1127 (1959).
10. Hill, D. E.: Phys. Rev. 114, 1414 (1959).
11. Baicker, J. A.: Phys. Rev. 129, 1174 (1963).
12. Wertheim, G. K.: Phys. Rev. 110, 1272 (1958).
13. Watkins, G. D.; and Corbett, J. W.: Phys. Rev. 121, 1001 (1961).
14. Fan, H. Y.; and Ramdas, A. K.: Proc. of the Int'l. Conf. on Semiconductor Physics, Prague, 309 (1960).
15. Corbett, J. W.; Watkins, G. D.; Chrenko, R. M.; and McDonald, R. S.: Phys. Rev. 121, 1015 (1961).
16. Ramdas, A. K.; and Fan, H. Y.: Jour. Phys. Soc. Japan. 18, Supp. II, 33 (1963).
17. Spitzer, W. G.; and Fan, H. Y.: Phys. Rev. 109, 1011 (1958).

18. Cheng, Li-Jen: PhD Thesis, Renesselaer Polytechnic Institute, Troy, New York, (1966).

19. Moss, T. S.: Optical Properties of Semiconductors, Butterworth and Co. Ltd. (1961).

20. Kaiser, W.; Keck, P. H.; and Lange, C. F.: Phys. Ref. 101, 1264 (1956).

21. Richards, R. E.; and Burton, W. R.: Trans. Faraday Soc. 45, 874 (1949).

22. Vavilov, V. S.: Effects of Radiation on Semiconductors; Consultants Bureau Enterprises, Inc., 1965.

23. Watkins, G. D.; and Corbett, J. W.: Phys. Rev. 138A, 543 (1965).

VITA

Gerald Franklin Hill

The author was born in New Bern, North Carolina, December 9, 1939. He attended Brinson Memorial Elementary School in Craven County, North Carolina, from September 1946 to June 1953. The author attended Dublin High School, Dublin, Georgia, and graduated from same in June 1958. He received a Bachelor of Science Degree in Nuclear Engineering from North Carolina State Univeristy, Raleigh, North Carolina, June 1962.

On June 18, 1962, the author began employment with the National Aeronautics and Space Administration, Langley Research Center, Hampton, Virginia.

In September 1963, the author enrolled at the College of William and Mary as a graduate student in Physics.

TABLE 1

DATA FOR SILICON SAMPLES IRRADIATED WITH 22 MeV PROTONS (ORNL)

SAMPLE NUMBER	TYPE	INITIAL RESISTIVITY (ohm-cm)	THICKNESS (mm)	OXYGEN CONCENTRATION $\times 10^{17}$ $\frac{O_2 \text{ Atoms}}{cm^3}$	INTEGRATED FLUX $\times 10^{16}$ protons/cm^2
422P	N	10	1.96	4.87	2.23
522P	P	1	2.01	2.59	2.23
622P	P	10	1.96	3.87	2.23
722P	N	1	1.93	4.84	2.23
822P	N	10	1.93	6.65	2.23
D	P	100	.79	12.5	2.23
M	P	1	3.63	7.27	1.18
N	N	10	3.63	5.87	1.02

TABLE 2

SUMMARY OF OXYGEN CONCENTRATION CALCULATIONS

SAMPLE NUMBER	$\alpha_{max}(9\mu)$	ΔH (cm^{-1})	ΔH (μ)	ΔH $(\times 10^{-3} ev)$	OXYGEN CONCENTRATION $\times 10^{17}$ $\frac{O_2 Atoms}{cm^3}$
422 P	5.26	22	454.5	2.73	4.87
522 P	3.61	17	588.2	2.11	2.59
622 P	3.99	23	434.8	2.85	3.87
722 P	4.64	25	400.	3.10	4.84
822 P	5.24	30	333.3	3.73	6.65
D	12.34	24	416.7	2.98	12.5
M	6.91	25	400.	3.10	7.27
N	5.79	24	416.7	2.98	5.87

TABLE 3

SUMMARY OF DEFECT LEVELS REPORTED

LOCATION OF INCREASED ABSORPTION (MICRONS)	ASSOCIATED DEFECT ENERGY LEVEL	REMARKS
1.8	E_c - 0.21 ev	DIVACANCY (refs. 9, 18).
3.46 3.62	E_c - 0.21 ev	Excited states of defect giving rise to the 1.8 micron absorption (refs. 9, 18).
11.6	———	Associated with oxygen vacancy complex (ref. 15).
12.0	E_c - 0.17 ev	Oxygen vibrational band composed of a substitutional oxygen atom coupled to a vacancy (A-center) (ref. 15).
12.67	———	Associated with oxygen vacancy complex (ref. 15).

TABLE 4

SOME PHYSICAL PROPERTIES OF SILICON

PROPERTIES	VALUE
Atoms per cm^3 (x 10^{22})	4.99
Band gap (25° C)(eV)	1.106
Debye temperature (°K)	652
Density (gm/cm^3)	2.328
Dielectric constant	11.7
Distance between nearest atoms (Å)	2.35
Elastic moduli (C_{11}) (x 10^{12}dynes/cm^2)	1.674
(C_{12})	.652
(C_{44})	.796
Electron effective mass ratio	1.1
Electron lattice mobility (cm^2/V . sec)	1900
Emissivity (1200° C)	~.5
Energy gap transition type	indirect
Hole effective mass ratio	.59
Hole lattice mobility (cm^2/V . sec)	425
Intrinsic electrons (25° C) (cm^{-3})	1.5×10^{10}
Intrinsic resistivity (25° C) (ohm-cm)	2.3×10^5
Latent heat of fusion (Kcal/mole)	9.45
Lattice constant (Å)	5.431
Magnetic Susceptibility (c.g.s.)	-0.13×10^{-6}
Melting Point (°C)	1420
Pressure at m.p. (atm)	10^{-6}
Refractive index, N	3.42
Specific heat (cal/gm)	0.181
Temp. dep. of band gap (eV/°C)	-4.4×10^{-4}
Temp. dep. of electron mobility	$T^{-2.5}$
Temp. dep. of hole mobility	$T^{-2.7}$
Thermal coeff. of expansion (1°)	4.2×10^{-6}
Thermal conductivity (watt units)	.84
Volume compressibility (x $10^{-12}cm^2$/degree	.98
Work function (eV)	5.05

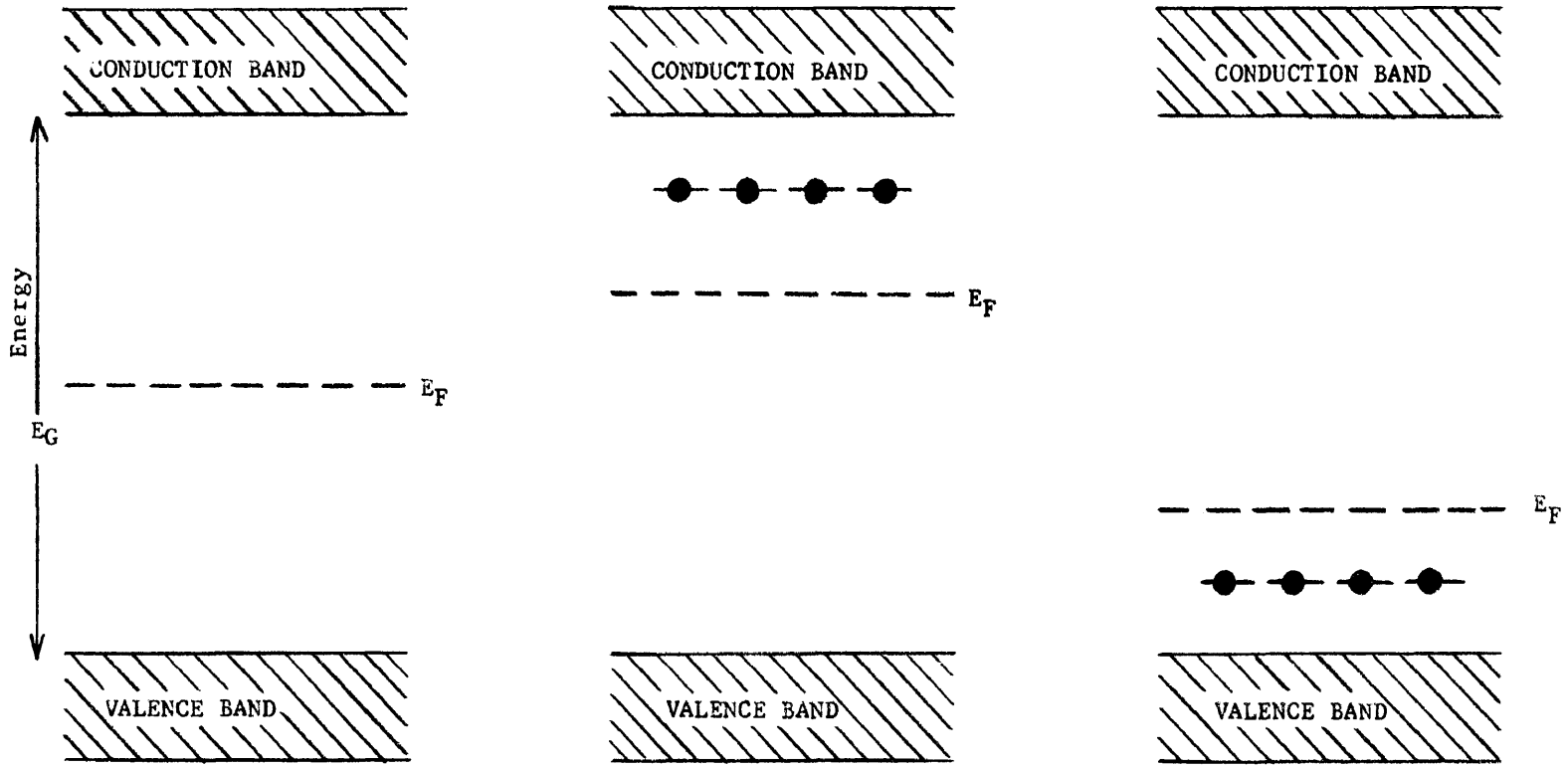

Figure 1.- Energy levels in semiconductors; (a) intrinsic, (b) N-type, and (c) P-type.

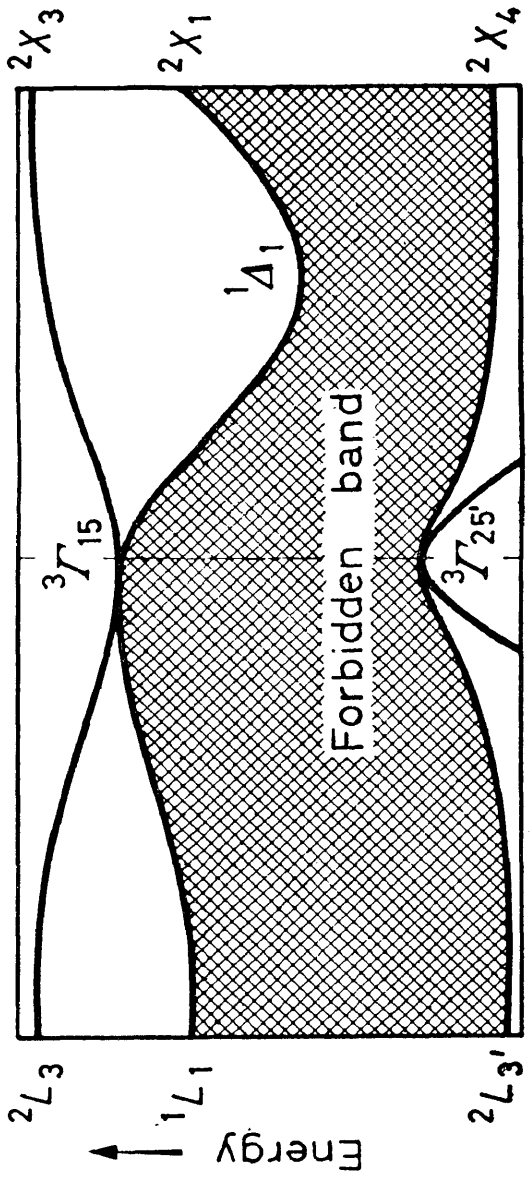

Figure 2.- Energy band structure of a silicon semiconductor.

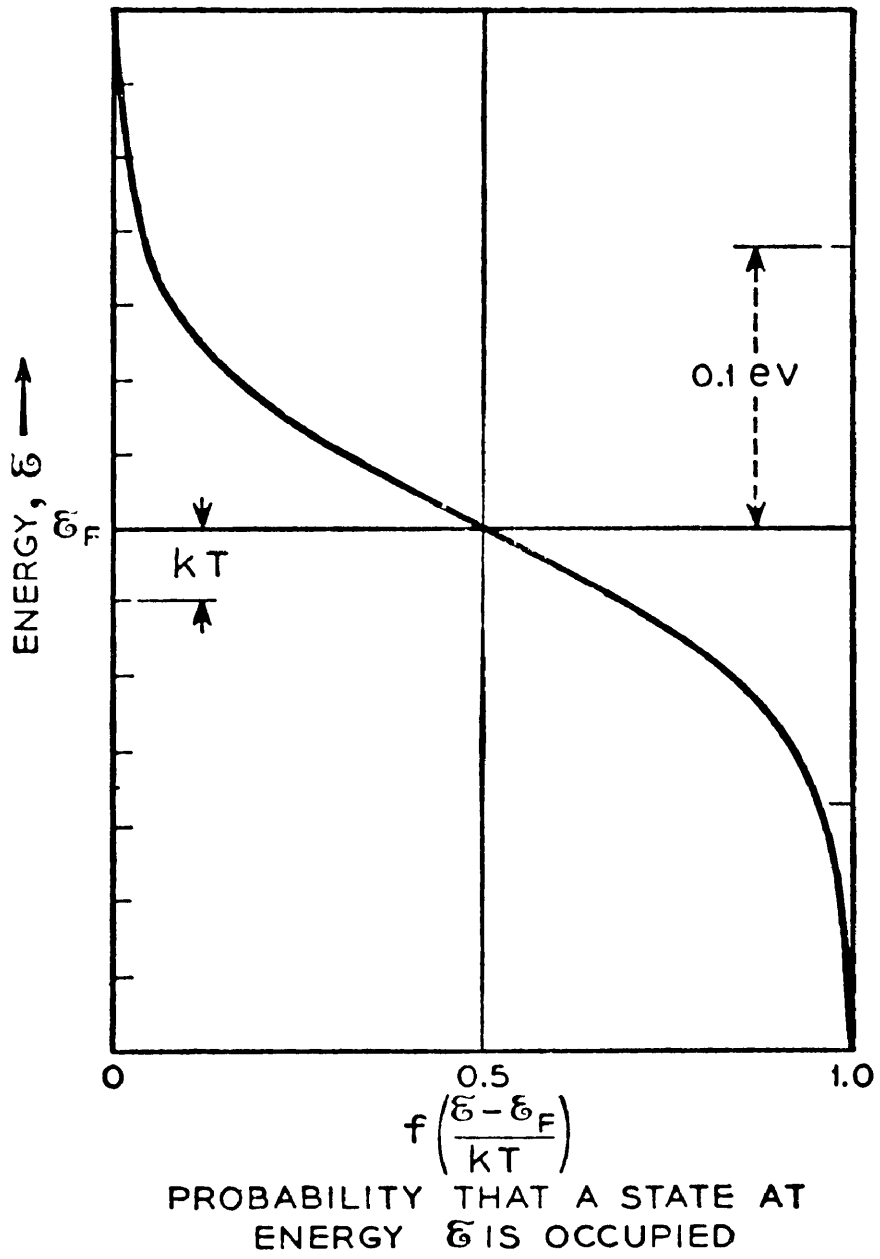

Figure 3.- Fermi-Dirac distribution function.

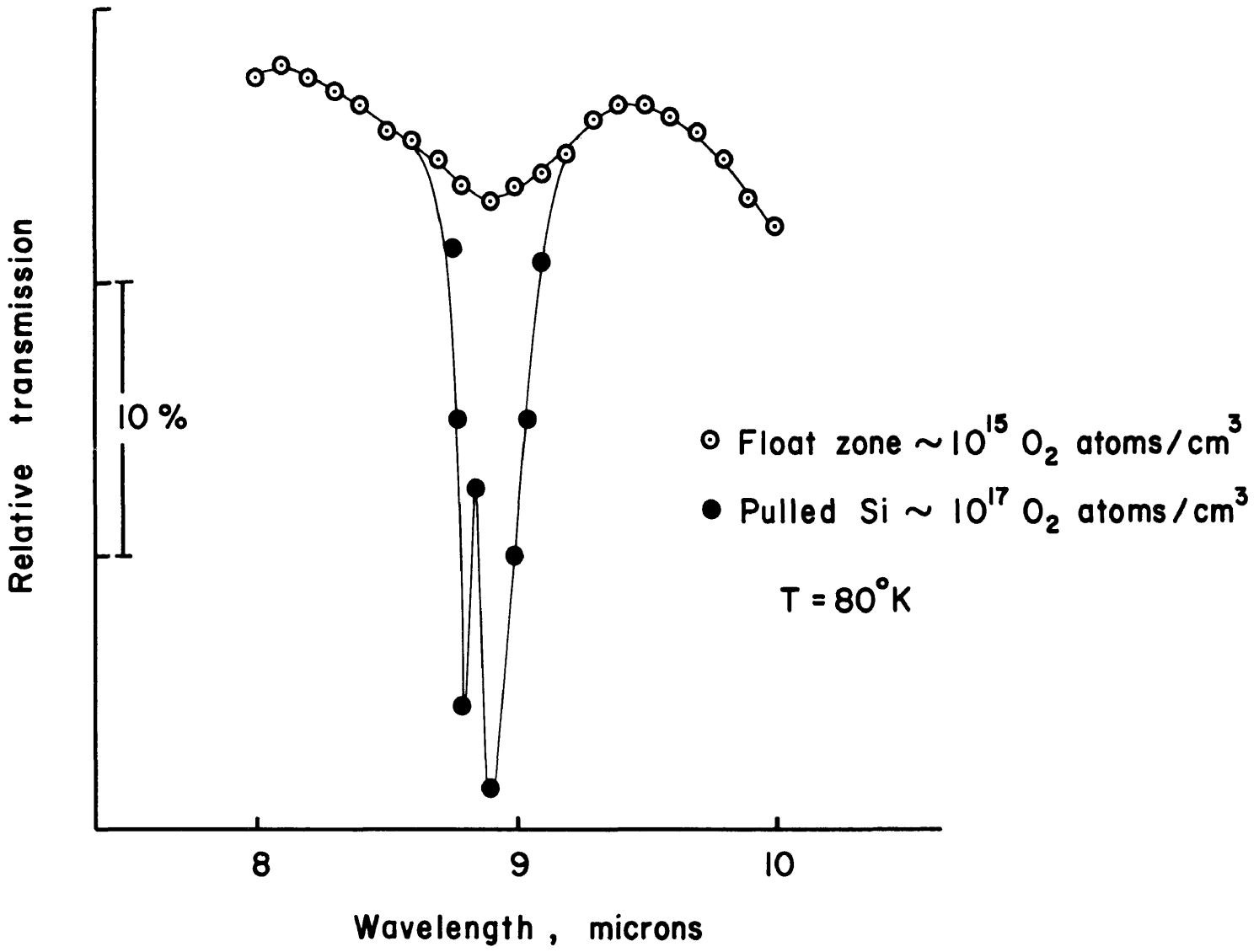

Figure 4.- Comparison of the infrared transmission of float zone and pulled silicon.

Figure 5.- The IR-9 infrared spectrometer and associated equipment used to obtain infrared spectra.

Figure 6.- DK-1A spectrometer used for making transmission spectra from 0.75 - 2.5 microns.

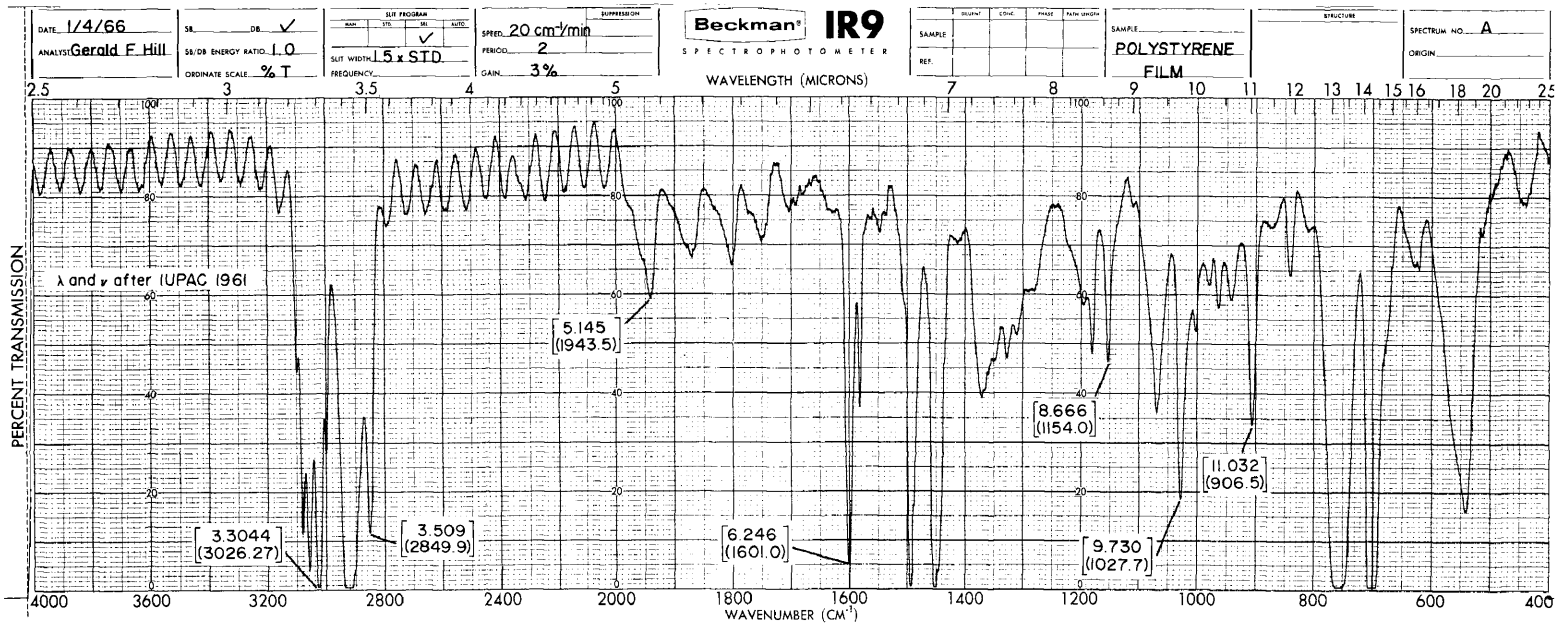

Figure 7.- Calibration spectrum of polystyrene film made on IR-9 spectrometer. Numbers in parentheses refer to wavenumber scale.

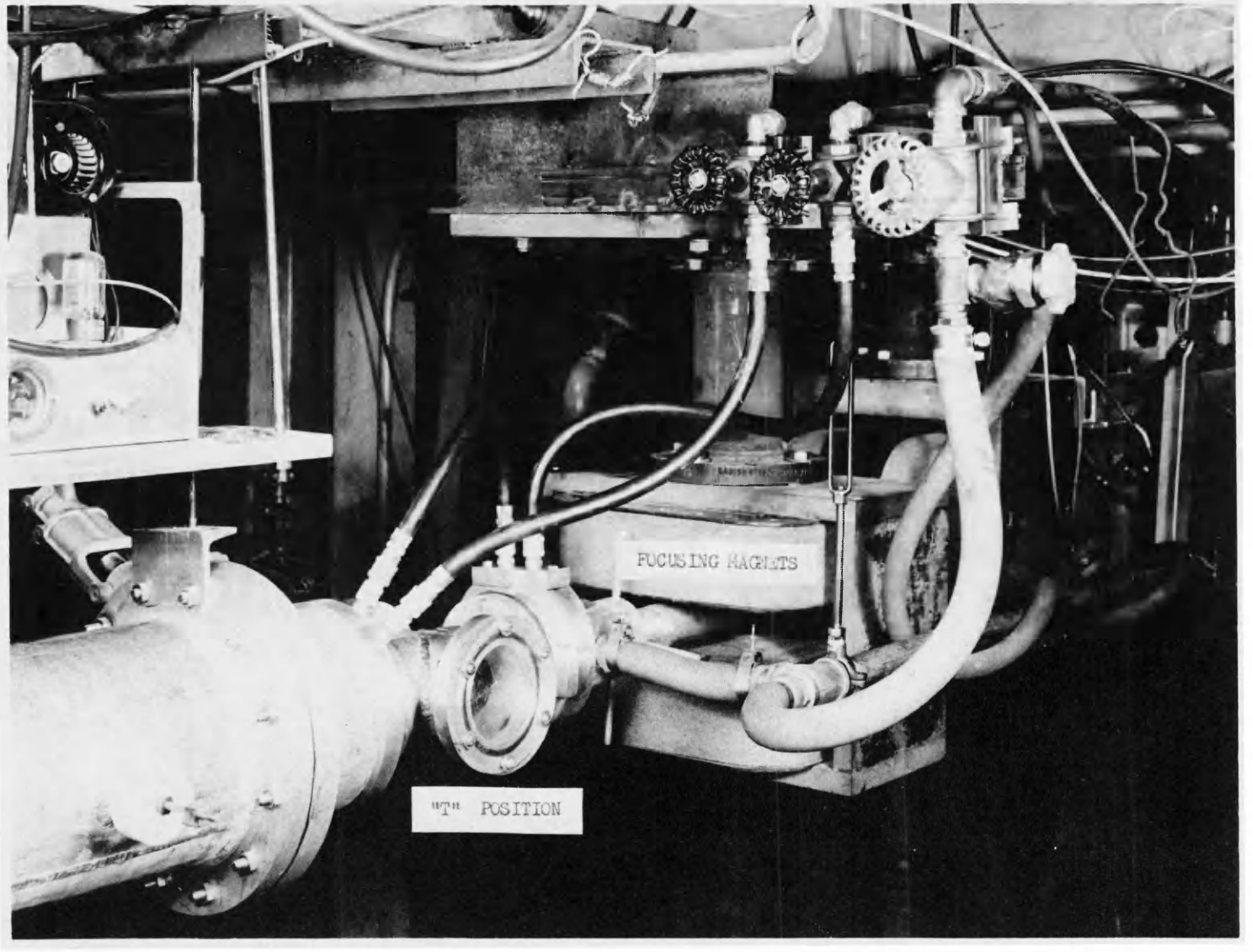

Figure 8.- "T" position of the 86 inch cyclotron at the ORNL.

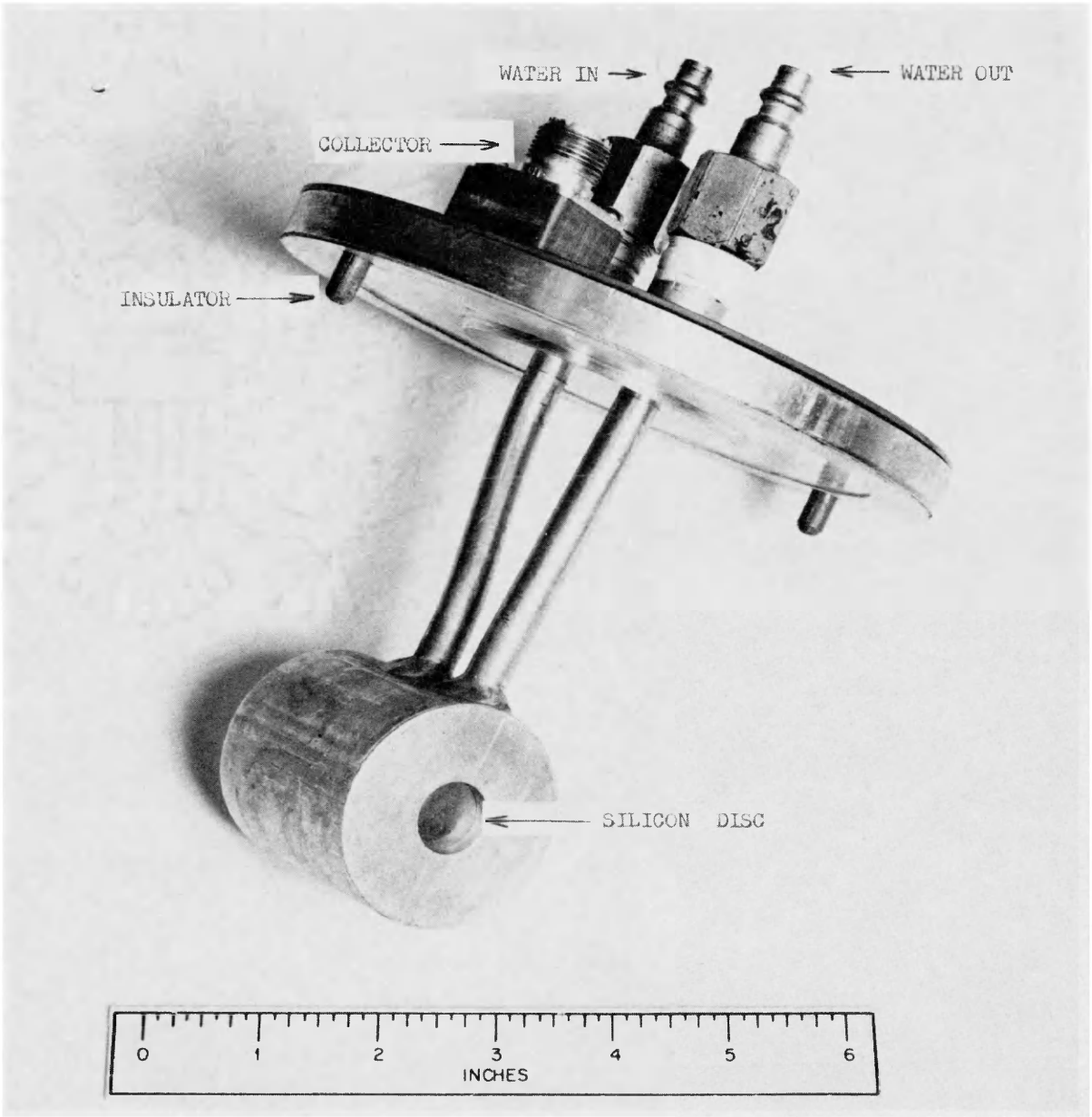

Figure 9.- Sample probe used to hold silicon disc into position in the proton beam pipe.

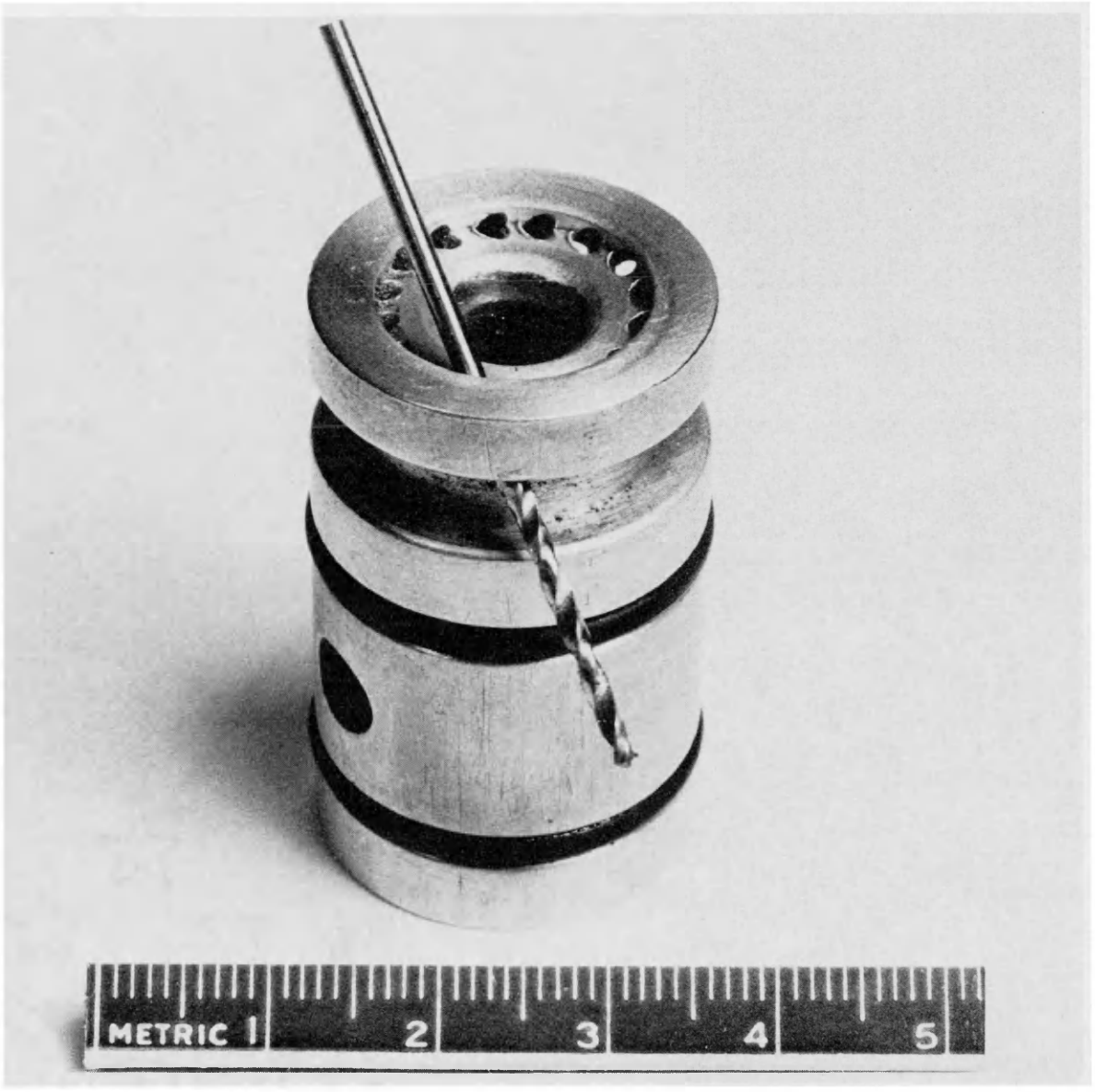

Figure 10.- Spiral water flow assembly used to water cool and hold silicon disc into sample probe.

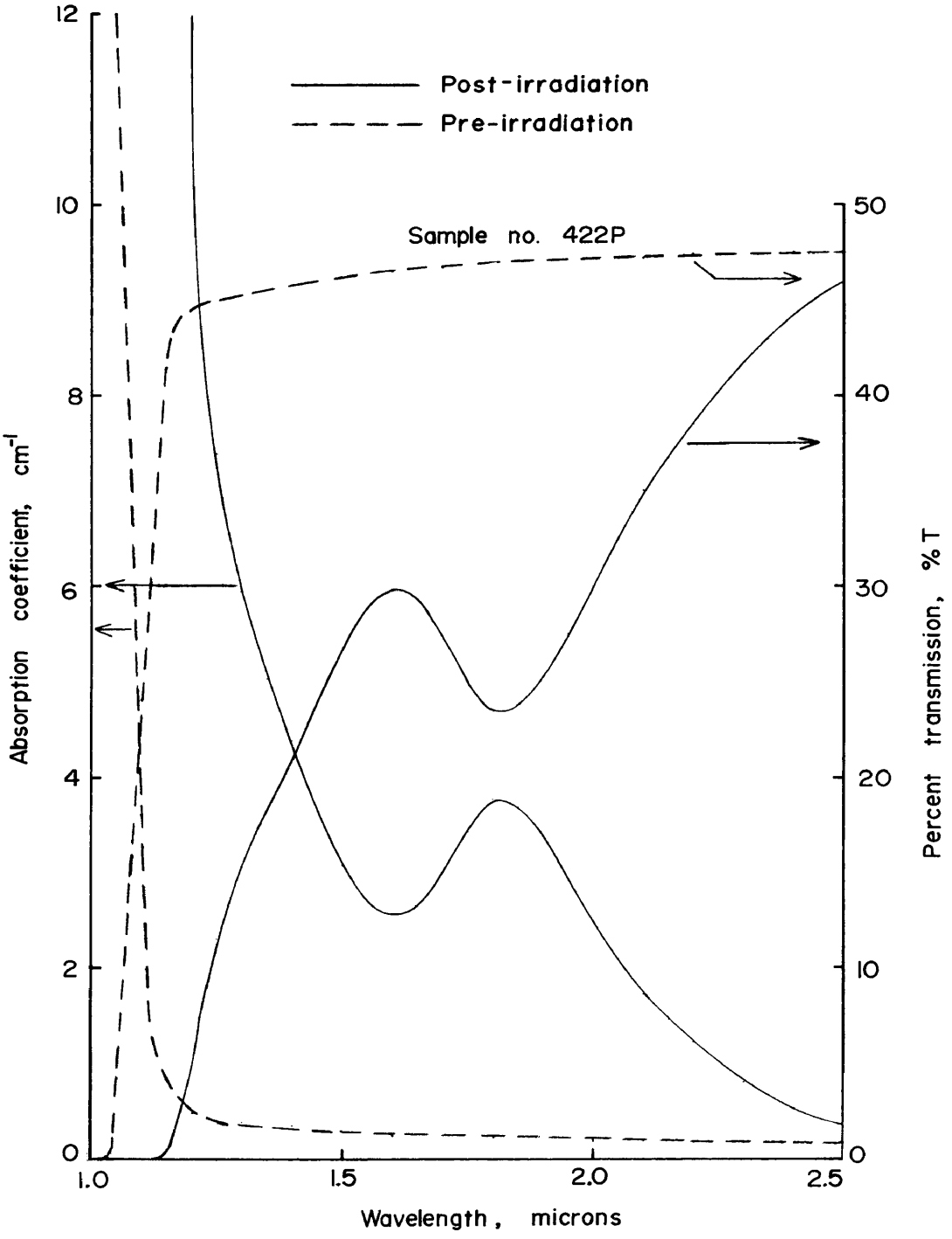

Figure 11.- The infrared transmission spectrum of an N-type, 10.0 ohm-cm silicon sample (No. 422P) exhibiting the 1.8 micron absorption peak at room temperature.

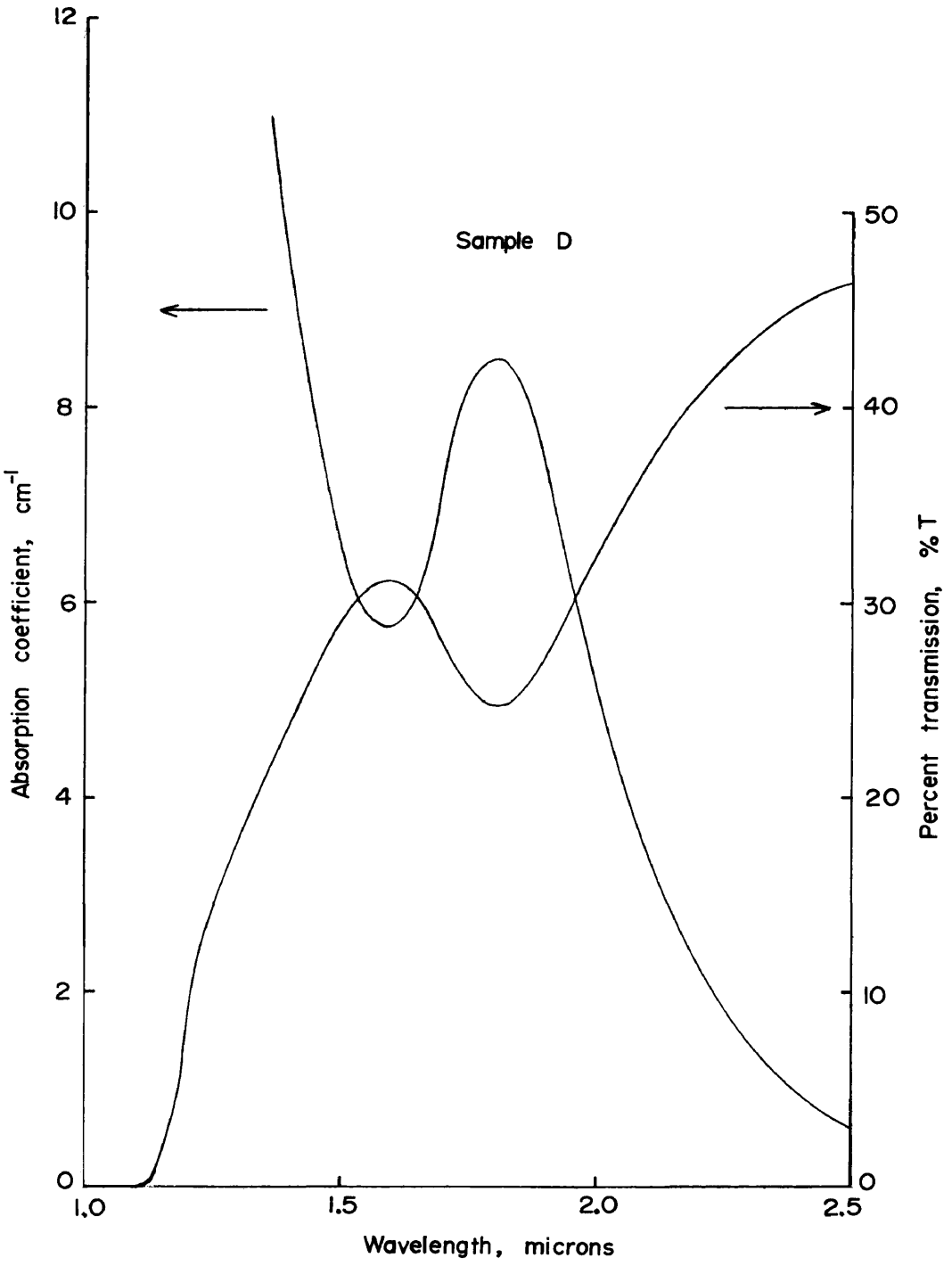

Figure 12.- The infrared transmission spectrum of a P-type, 100.0 ohm-cm silicon sample (No. D) exhibiting the 1.8 micron absorption peak at room temperature.

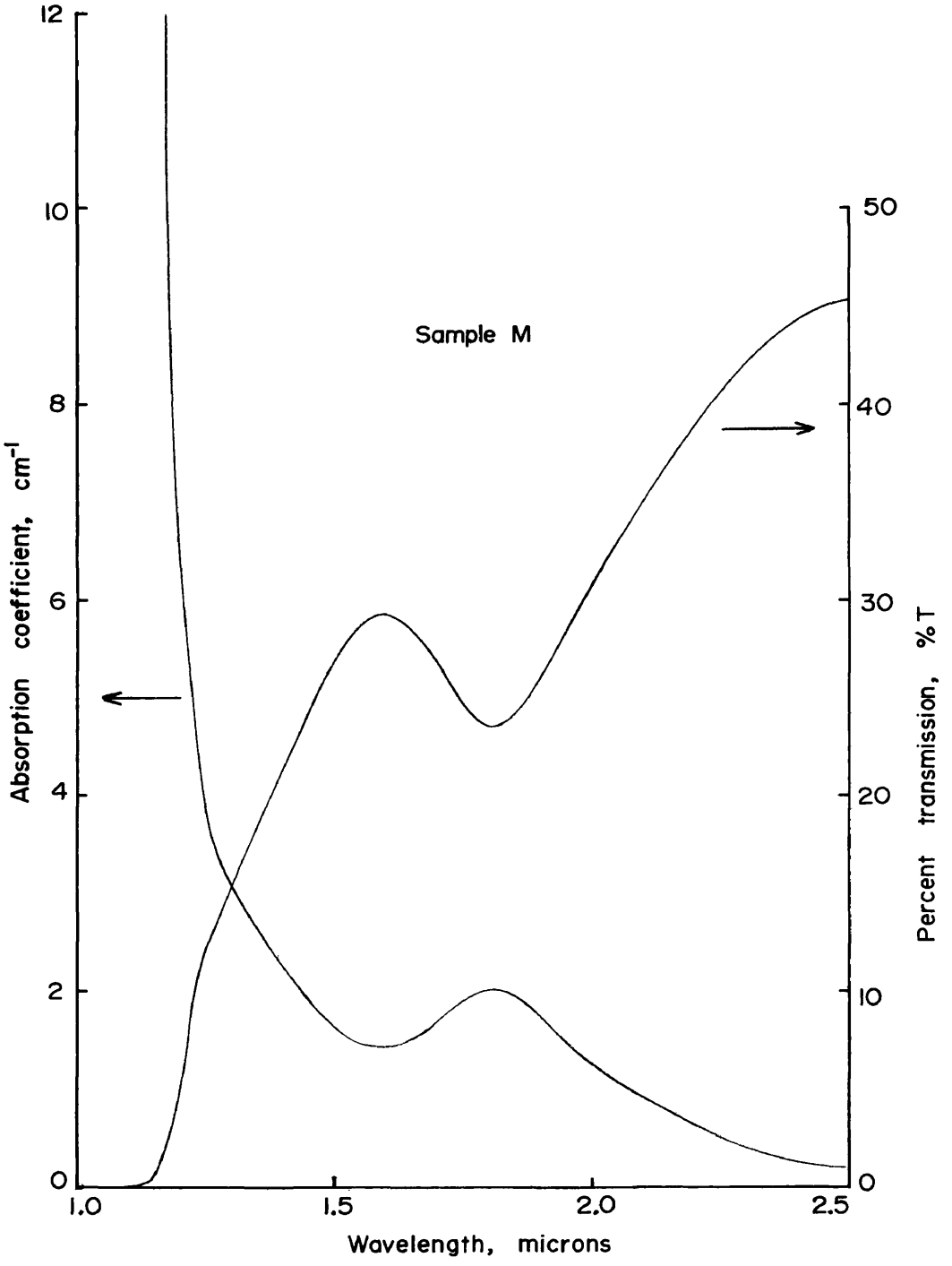

Figure 13.- The infrared transmission spectrum of a P-type, 1.0 ohm-cm silicon sample (No. M) exhibiting the 1.8 micron absorption peak at room temperature.

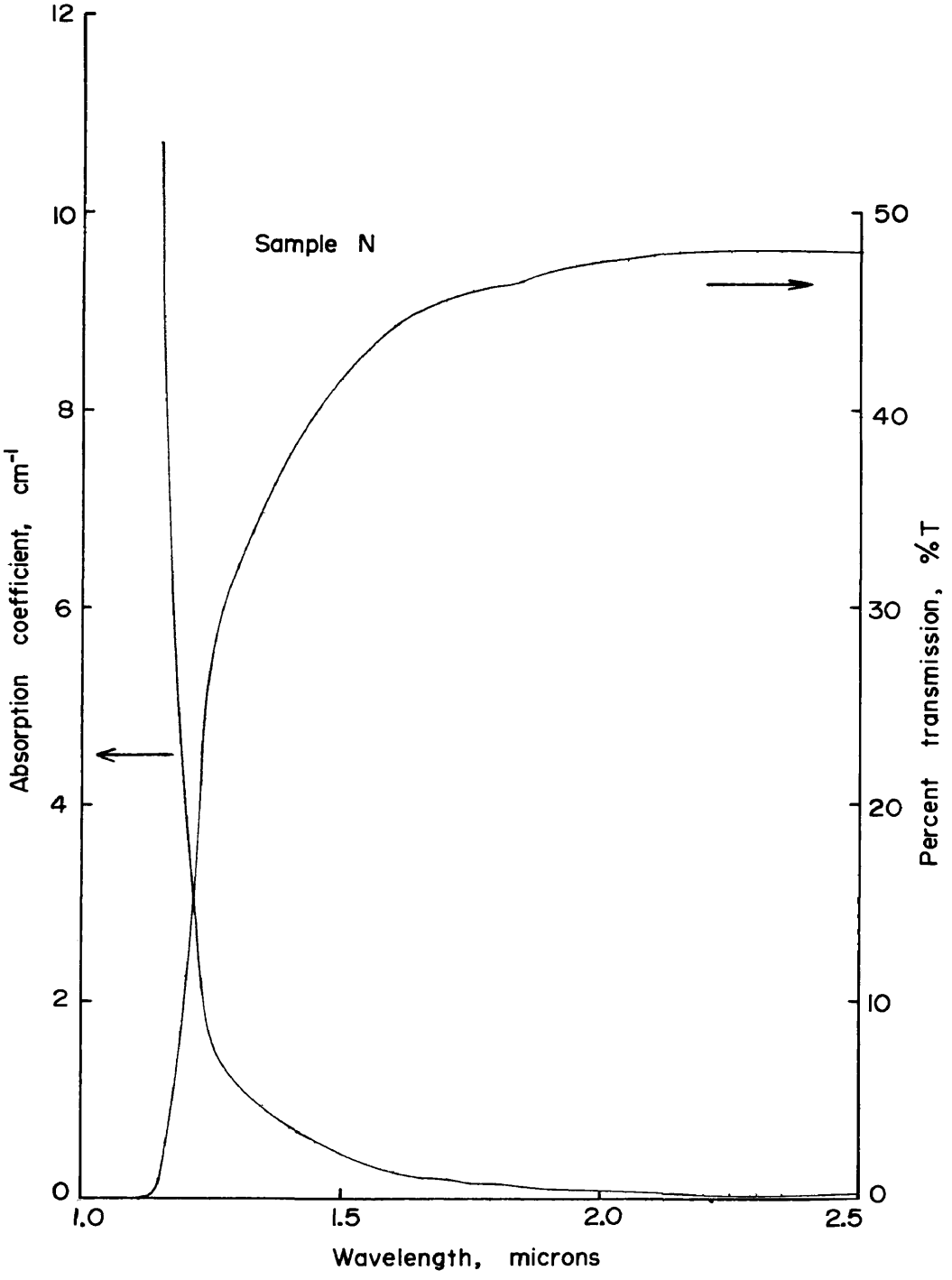

Figure 14.- The infrared transmission spectrum of an N-type, 10.0 ohm-cm silicon sample (No. N) exhibiting the absence of the 1.8 micron absorption peak at room temperature.

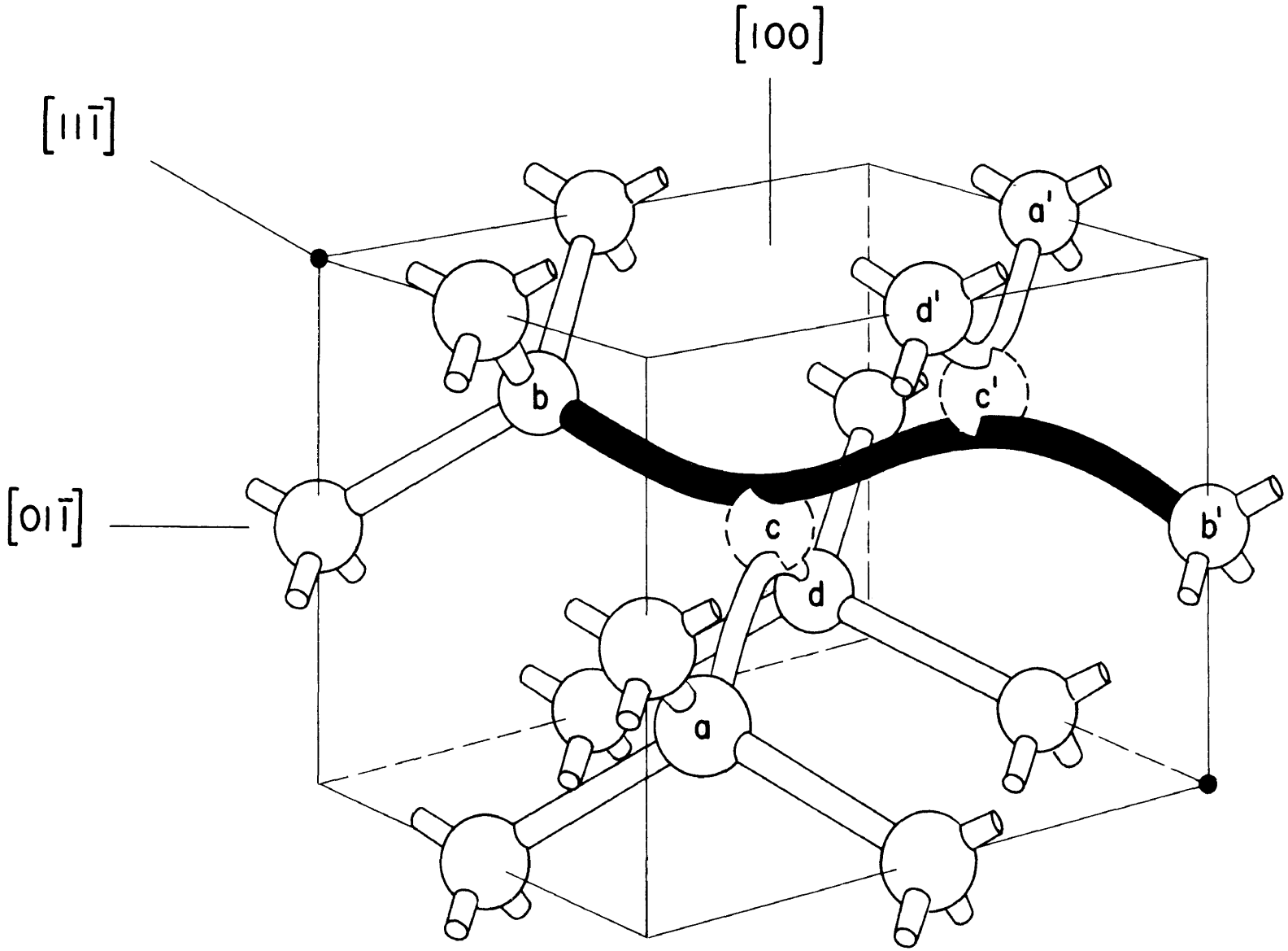

Figure 15.- A model of the divacancy showing the crystal orientation (ref. 18).

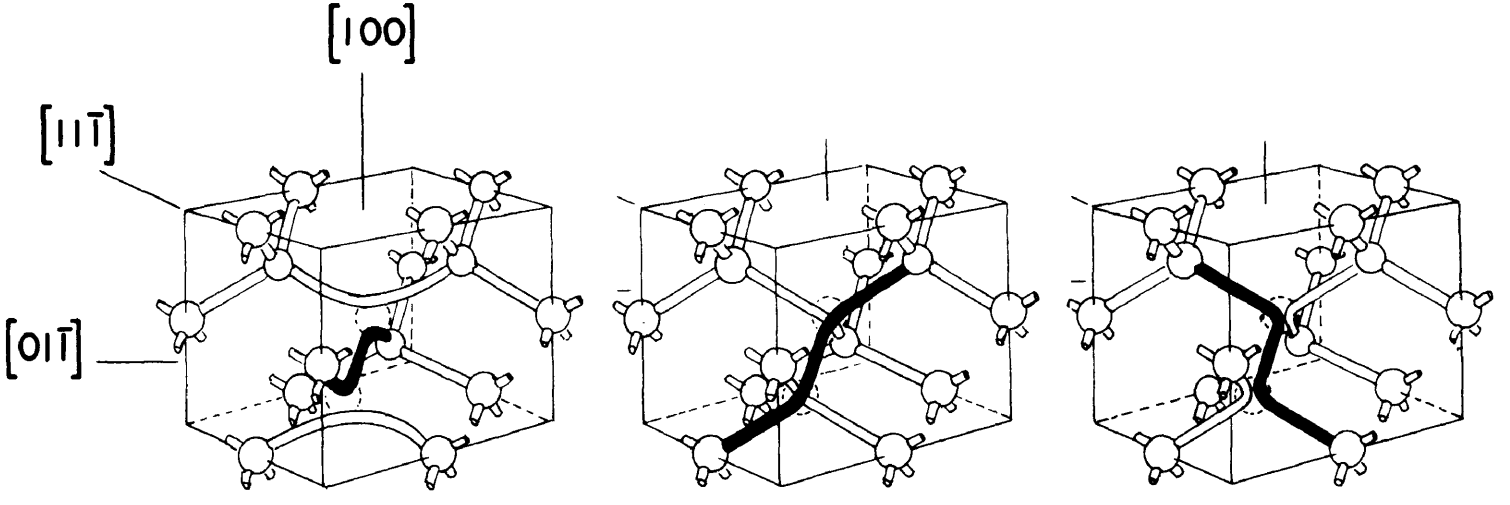

Figure 16.- Three equivalent electronic distributions of a divacancy (ref. 18). The orientations of the sample are shown.

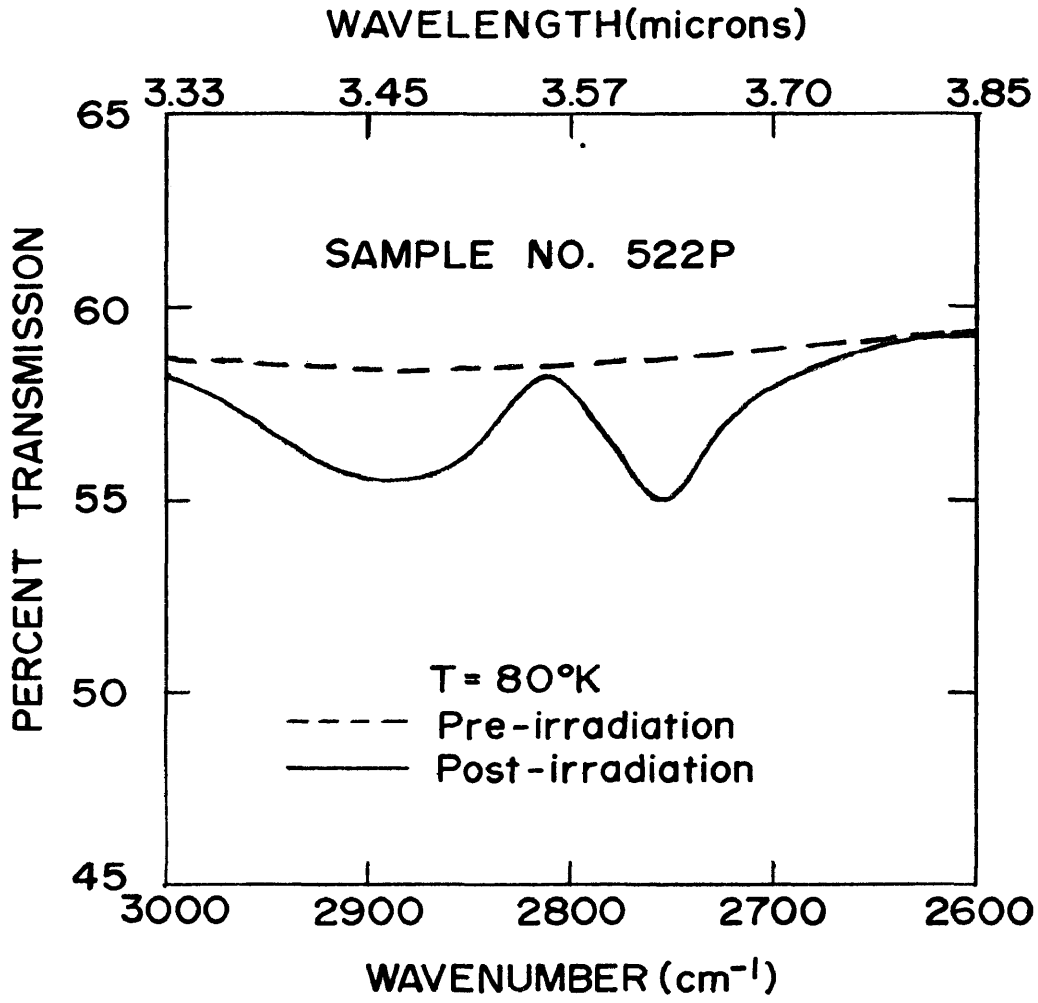

Figure 17.- The infrared transmission spectrum of a P-type, 1.0 ohm-cm silicon sample (No. 522P) exhibiting the 3.46 and 3.62 absorption peaks at liquid nitrogen temperature.

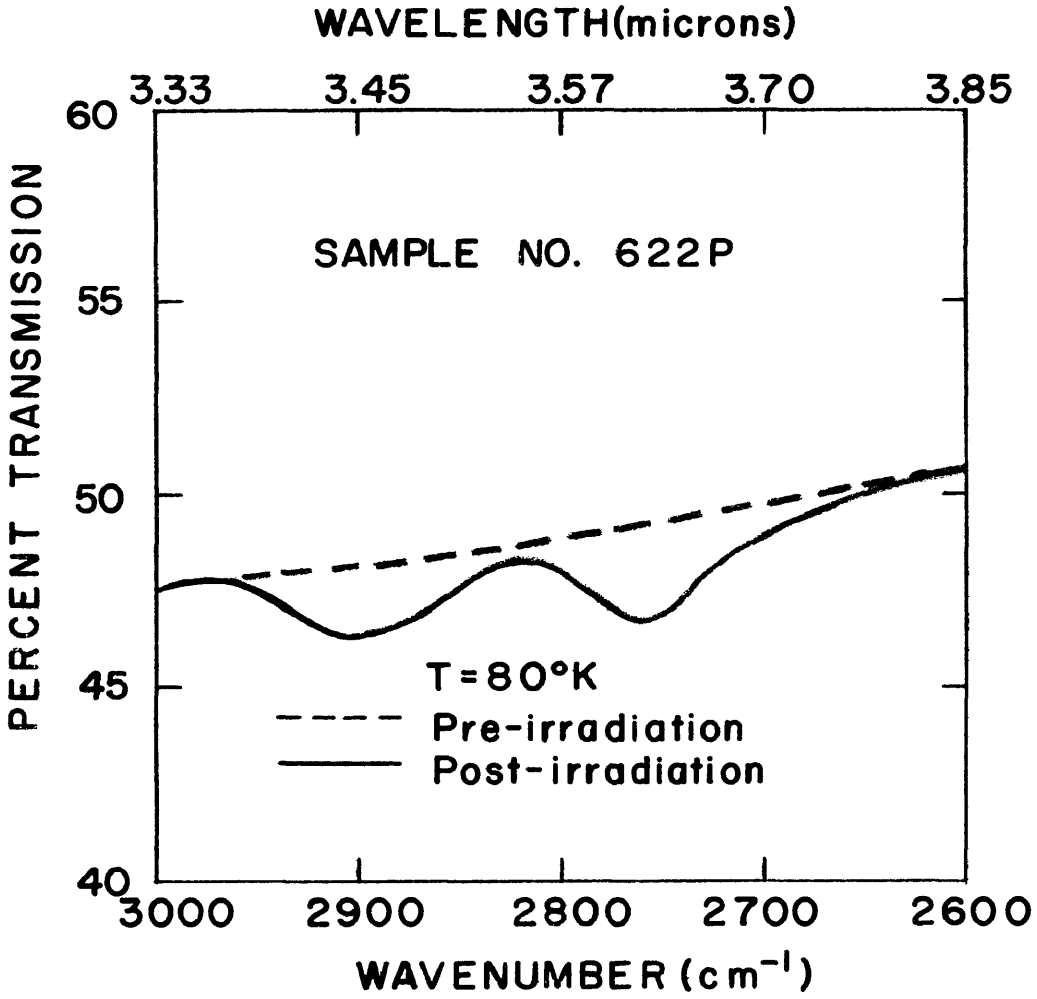

Figure 18.- The infrared transmission spectrum of a P-type, 10.0 ohm-cm silicon sample (No. 622P) exhibiting the 3.46 and 3.62 absorption peaks at liquid nitrogen temperature.

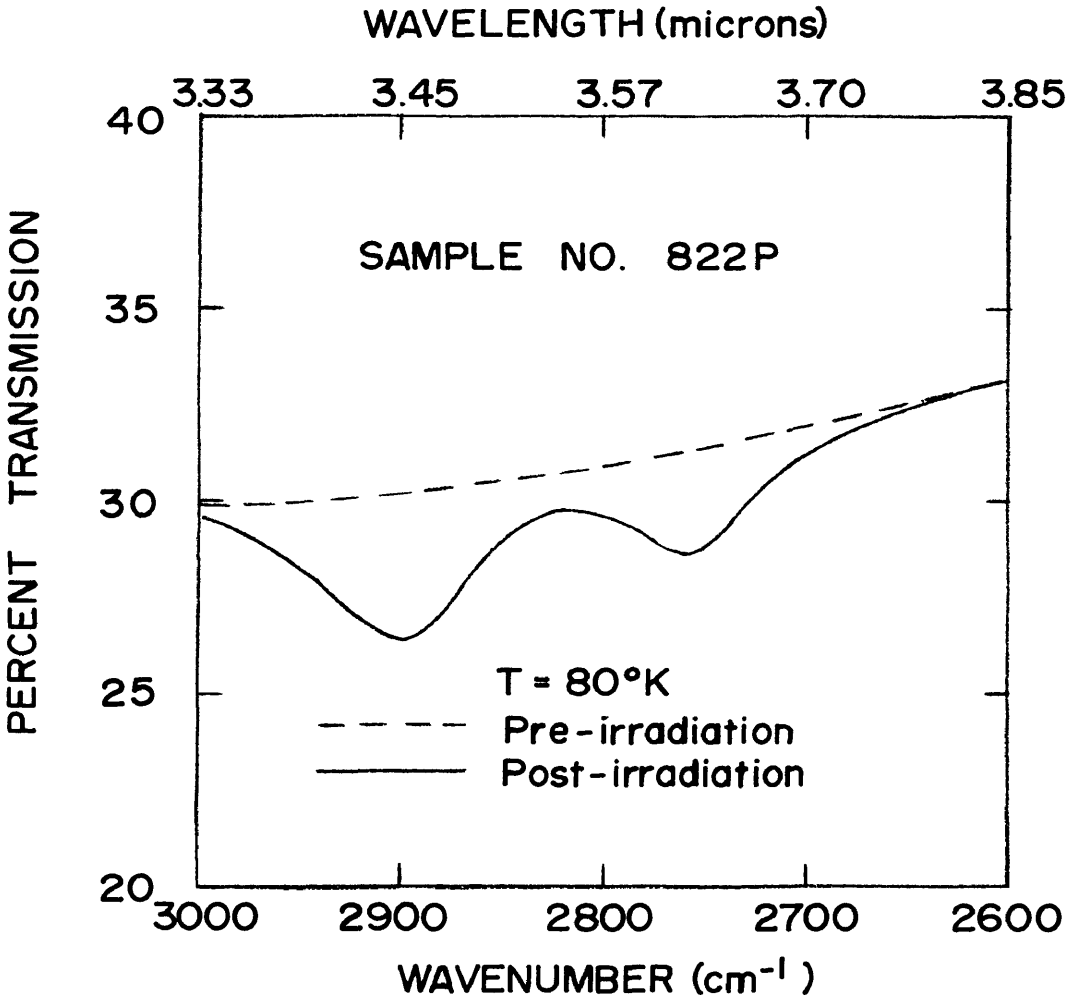

Figure 19.- The infrared transmission spectrum of an N-type 10.0 ohm-cm silicon sample (No. 822P) exhibiting the 3.46 and 3.62 micron absorption peaks at liquid nitrogen temperature.

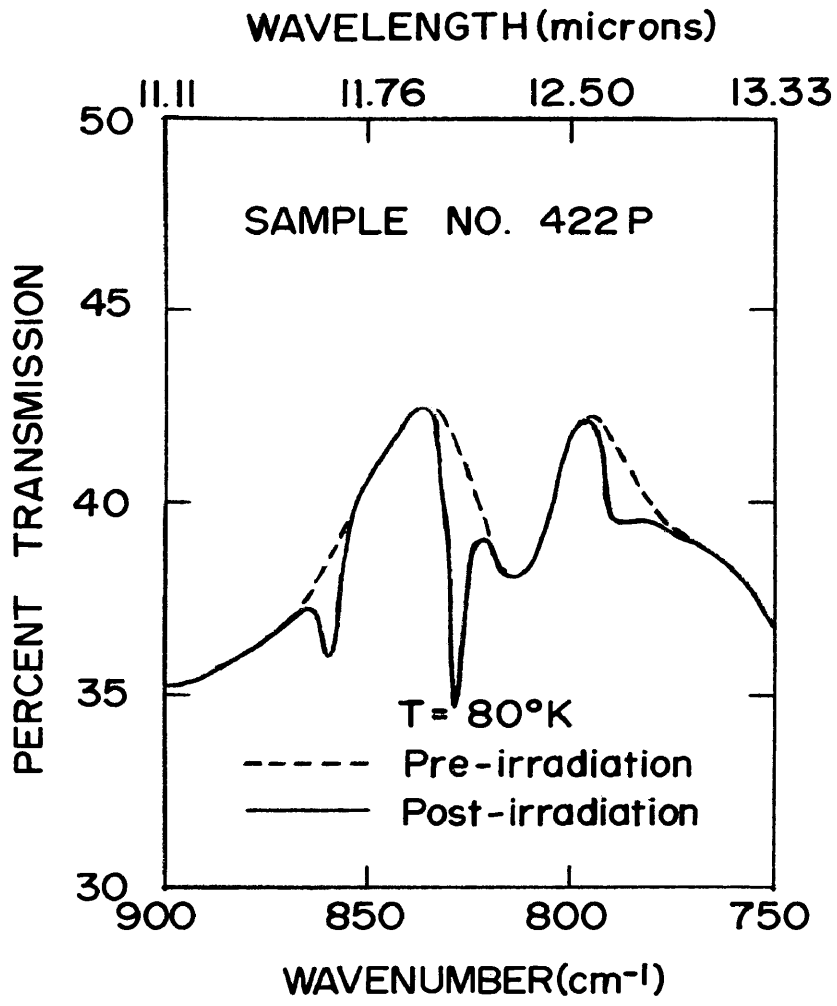

Figure 20.- The infrared transmission spectrum of an N-type 10.0 ohm-cm silicon sample (No. 422P) exhibiting the 11.6, 12.0, and 12.67 micron absorption peaks at liquid nitrogen temperature.

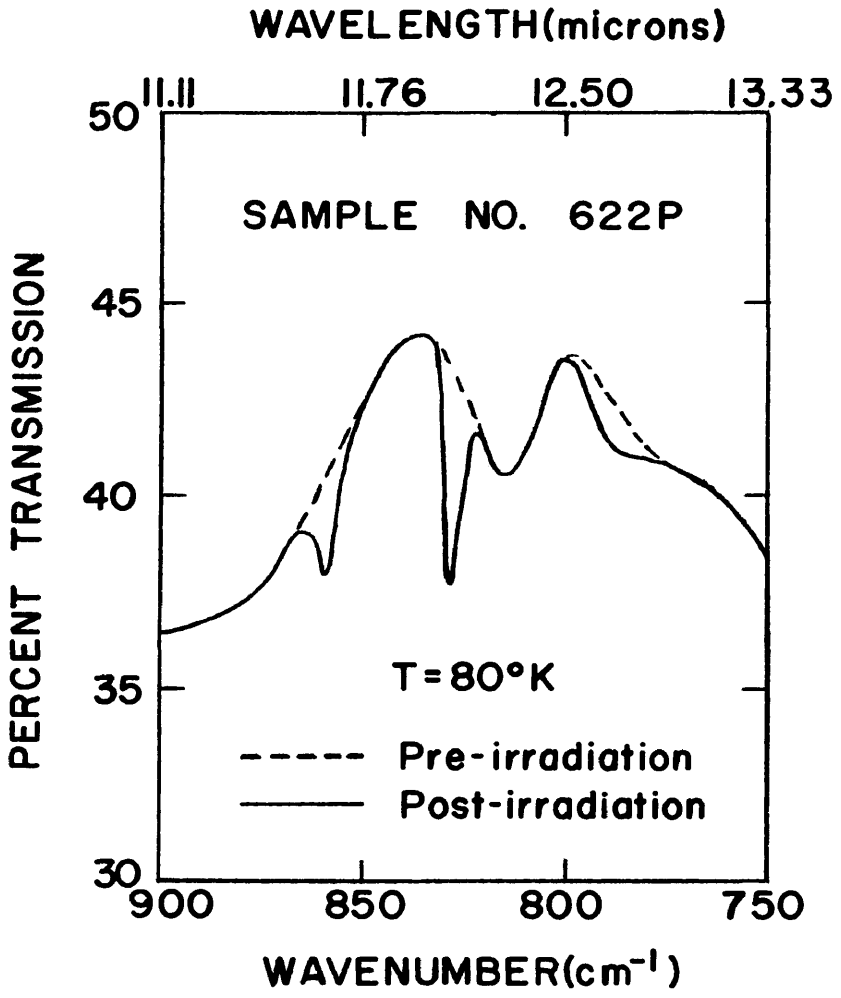

Figure 21.- The infrared transmission spectrum of a P-type, 10.0 ohm-cm silicon sample (No. 622P) exhibiting the 11.6, 12.0, and 12.67 micron absorption peaks at liquid nitrogen temperature.

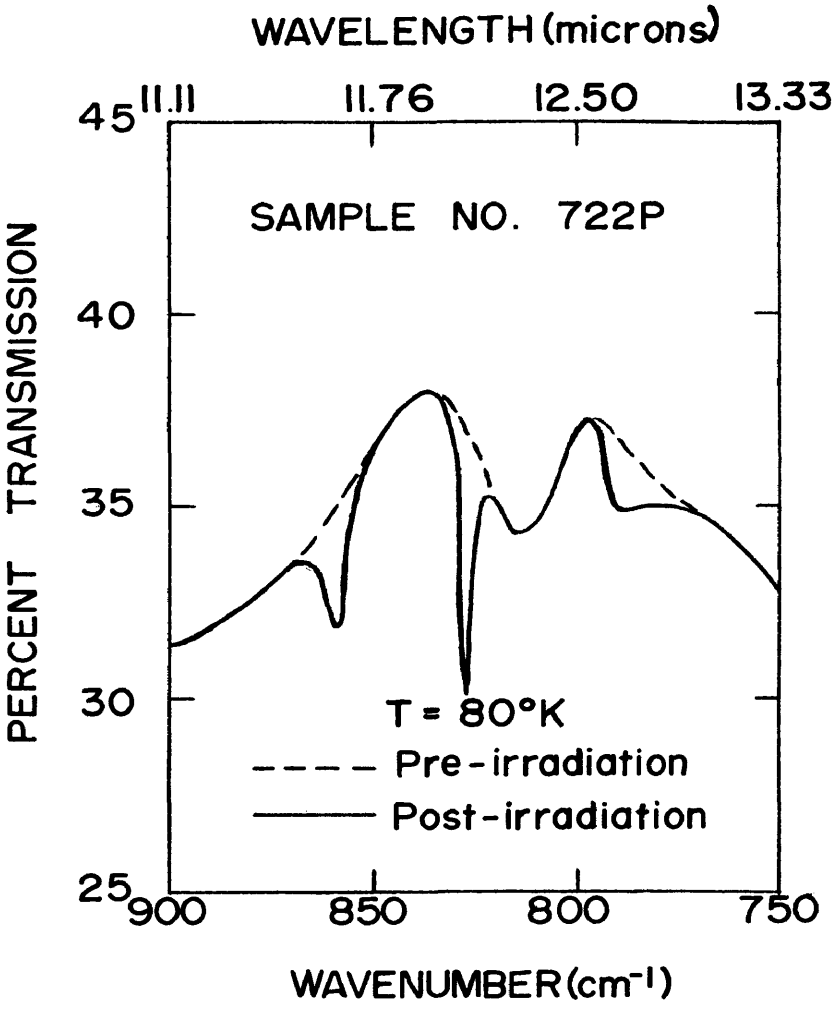

Figure 22.- The infrared transmission spectrum of an N-type, 1.0 ohm-cm silicon sample (No. 722P) exhibiting the 11.6, 12.0, and 12.67 micron peaks at liquid nitrogen temperature.

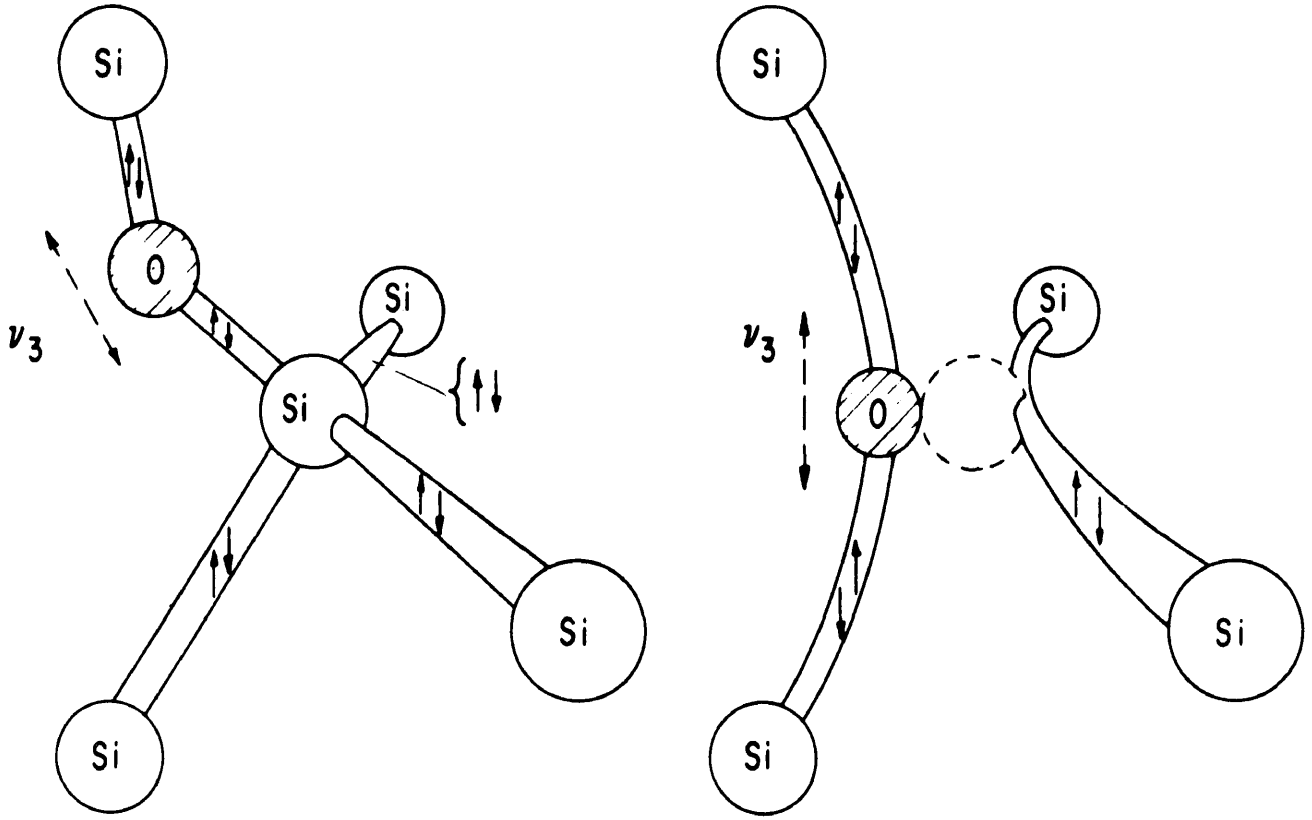

Figure 23.- Configuration of the nonlinear Si-O-Si molecule for (A) the case where the oxygen is in the "interstitial" site which is associated with the 9 micron band and (B) the case where the oxygen is in the "substitutional" site which is associated with the 12 micron band and the silicon - A center. The ν_3 dipole moment direction is indicated (ref. 15).

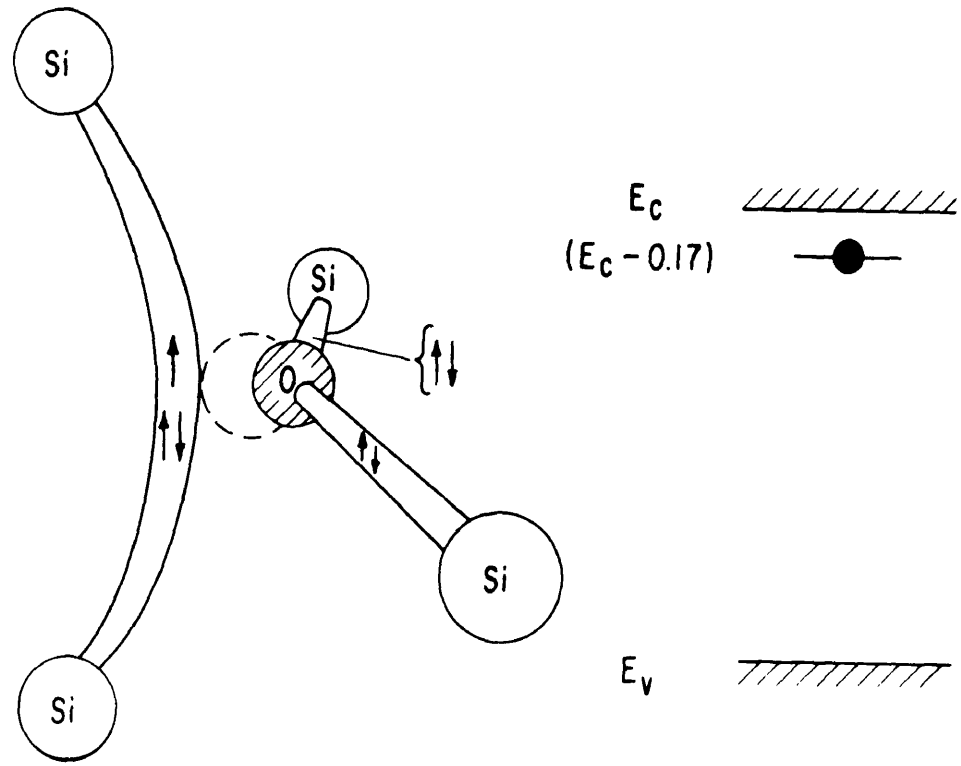

Figure 24.- Model of the silicon - A center showing the unpaired electron (ref. 15). The associated electrical level is at $(E_c - 0.17eV)$.